Recombinant Expression and Functional Characterization of Human Hephaestin: A Multicopper Oxidase with Ferroxidase Activity

by

Tanya A. M. Griffiths

B.Sc., Malaspina University-College, 2000

A THESIS SUBMITTED IN PARTIAL FULFILMENT OF
THE REQUIREMENTS FOR THE DEGREE OF

DOCTOR OF PHILOSOPHY

in

THE FACULTY OF GRADUATE STUDIES

(Biochemistry and Molecular Biology)

THE UNIVERSITY OF BRITISH COLUMBIA
January 2006

Abstract

Human hephaestin is a transmembrane protein that has been implicated in duodenal iron export. Mutations in the murine *hephaestin* gene produce microcytic, hypochromic anemia that is refractory to oral iron therapy. Hephaestin shares ~50% sequence identity with the plasma multicopper ferroxidase ceruloplasmin including conservation of residues involved in disulfide bond formation and metal coordination. Based on this similarity to ceruloplasmin, human hephaestin may also bind copper and possess ferroxidase activity. To test this hypothesis, human hephaestin cDNA has been cloned by reverse transcription of human duodenal mRNA. Following *in vitro* mutagenesis to engineer the encoded polypeptide so that it was suitable for expression and purification, the cDNA was cloned into the expression vector pNUT and introduced into baby hamster kidney cells. After selection with methotrexate, the baby hamster kidney cells secreted the recombinant human hephaestin into the medium at a level of ~2 mg/L. Purification was achieved by a single immunoaffinity chromatography step. As judged by SDS-PAGE, N-terminal sequence analysis, and matrix assisted laser desorption ionization time-of-flight mass spectrometry, the purified hephaestin was homogeneous with a mass of 129,600 Da suggesting a carbohydrate content of ~7.7%. Inductively coupled plasma mass spectrometry revealed that recombinant hephaestin contained an average of 3.13 atoms of copper per protein molecule. A visible absorption maximum was observed at 607 nm that is consistent with the presence of a Type 1 copper site. By using ferrous ammonium sulfate as a substrate, recombinant hephaestin was shown to have ferroxidase activity with a K_m of 2.1 μM for Fe(II). Lastly, urea PAGE showed that hephaestin was able to oxidize Fe(II) to Fe(III) that was acceptable by apo transferrin to form diferric transferrin.

Table of Contents

List of Tables

List of Figures

List of Abbreviations

AAA	amino acid analysis
apo Tf	apo transferrin
BHK	baby hamster kidney
CAPS	N-cyclohexyl-3-aminopropanesulfonic acid
Cp	ceruloplasmin
DMEM	Dulbecco's modified Eagle medium-Ham F12
DMT-1	divalent metal transporter-1
DODAC	N,N-dioleyl-N,N-dimethylammonium chloride
DOPE	dioleoylphosphatidylethanolamine
ECL	enhanced chemiluminescence
Fpn1	ferroportin 1
FXa	Factor Xa
HCP1	heme carrier protein 1
HEK	human embryonic kidney
HFE	hereditary hemochromatosis protein
Hp	hephaestin
ICP MS	inductively coupled plasma mass spectrometry
IP	immunoprecipitation
LUV	large unilamellar vesicle
MALDI TOF MS	matrix assisted laser desorption ionization time-of-flight mass spectrometry
MCO	multicopper oxidase
NAPS	Nucleic Acid Protein Service

NCS	newborn calf serum
NHE	normal hydrogen electrode
NMWL	nominal molecular weight limit
PAGE	polyacrylamide gel electrophoresis
PBS	phosphate buffered saline
PCR	polymerase chain reaction
PVDF	polyvinylidene fluoride
RT-PCR	reverse transcriptase-polymerase chain reaction
SDS-PAGE	sodium dodecyl sulfate-polyacrylamide gel electrophoresis
sla	*sex-linked anemia*
T1(2,3)	type 1 (2,3) copper atoms
TBST	Tris buffered saline containing 0.05% Tween-20
Tf	transferrin
TfR	transferrin receptor

Acknowledgments

Completion of a Ph.D. is far from a solitary endeavor and my list of acknowledgments reflects this.

Dr. Ross MacGillivray – you have encouraged me when I've been discouraged and continually helped me to step out of my comfort zone and face new challenges. It has been a pleasure and a privilege to work with you.

Members of my supervisory committee: Dr. Grant Mauk, Dr. Dana Devine, and Dr. Elisabeth Maurer – thank you for your continued interest in my project and my future scientific endeavors. A special thank you to Grant for providing me with much of your time and wit.

Past and present colleagues in the MacGillivray lab – you have provided me with support, laughter, and advice. Each of you, in your own way, has made my time in the lab unforgettable. Val and Eve, what would I have done without you? A special thank you to Ann Wong for her contribution of Figure 1.1.

Dr. Susan Curtis and Laurie Molday – without both of you, this project would not have gotten off the ground! Thank you.

Influential instructors at my *alma mater* Malaspina University-College – thank you for setting me on the right foot for a graduate career!

Members of my family – I am so grateful for your emotional, spiritual, and financial support. Also, your understanding about my infrequent and short visits was much appreciated! Thanks for the pep talks, Mom!

My dear friends, Andrea Griffiths and Christine Mann – your encouragement, kindness, sense of humor, and fantastic listening skills have gotten me through some difficult times. Thank you both very much.

My wonderful husband, Brett Griffiths – you should receive an honorary Ph.D. as you've probably spent as much time in the lab as I have! I couldn't have asked for a more understanding and supportive husband. Thank you for teaching me about *d*-orbitals, helping with my lab equipment troubles, bouncing ideas around with me, and making me laugh!

This thesis is dedicated to the loving memory of my brother, Stevan Wood.

Chapter 1. Introduction

1.1 Iron Chemistry

Iron is the fourth most abundant element in the Earth's crust [1], yet despite this abundance, iron deficiency is prevalent in 66-80% of the world's population (World Health Organization Statistics, 2003). Much of the world's iron deficiency epidemic is due to malnutrition in developing countries, but even with an iron rich diet, only 10% of ingested iron is absorbed (compared with copper absorption, which is around 70%) [2]. Part of this relatively low absorption is due to the complex chemistry of Fe(III) in aqueous solutions that precludes its solubility at neutral pH. Aqueous iron is present in two major oxidation states, ferrous iron, Fe(II), and ferric iron, Fe(III). At low pH, both Fe(II) and Fe(III) are soluble as $[Fe(H_2O)_6]^{2+}$ and $[Fe(H_2O)_6]^{3+}$, respectively. However, as the pH is raised above 2.0, Fe(III) forms the insoluble $[Fe(H_2O)_3(OH^-)_3]$ complex. Also, in the presence of physiological oxygen concentrations, Fe(II) will auto-oxidize to Fe(III) and thus contribute to the insolubility of iron at neutral pH [3]. This phenomenon illustrates the need for ligands to increase the solubility of iron at physiological oxygen tensions and pH; common biological ligands of dietary iron are citrate and amino acids such as histidine [4].

The Fe(II)/Fe(III) redox couple is very reactive and participates in a variety of biological processes involving single electron transfer reactions. This reactivity, paired with the fact that iron is the most abundant transition metal on Earth [1], makes iron essential in biological systems. However, the reactivity comes at a cost as single electron transfer reactions may lead to formation of oxygen and hydroxyl radicals via the Haber-Weiss-Fenton series of reactions:

$$Fe^{2+} + O_2 \rightarrow Fe^{3+} + O_2^{\cdot\cdot}$$

$$2O_2^{\cdot\cdot} + 2H^+ \rightarrow H_2O_2 + O_2$$

$$Fe^{2+} + H_2O_2 \rightarrow OH^{\cdot} + OH^- + Fe^{3+}$$

The superoxide radical has been shown to oxidize iron-sulfur clusters, and the release of iron from these clusters propagates the formation of hydroxyl radicals [5]. The hydroxyl radical can cause oxidative damage to many essential cellular components including nucleic acids, lipids, and proteins [6].

1.2 Prokaryotic Iron Metabolism

Prokaryotic organisms have an obligatory requirement for iron, as do most other organisms. Thus, several mechanisms exist to promote iron uptake in an environment where much of the iron exists as the insoluble Fe(III) species or is already bound to chelators or other iron-containing molecules. Of interest, but outside the scope of this Introduction, are members of the *Lactobacillus* genus – these bacteria are iron-independent and live in iron-limited environments such as milk or in the gut of breast-fed infants [7]. The majority of bacterial species obtain iron in one of two ways: by direct contact with an iron source or by an indirect method mediated by siderophores or hemophores. If Fe(II) is present in the environment, it is readily taken up by cell surface transporters found in Gram negative bacteria. Both Gram positive and Gram negative bacteria can sequester iron from mammalian iron-binding proteins, such as transferrin and lactoferrin. Many of the heme containing proteins such as hemoglobin and hemopexin are recognized and taken up by a

variety of bacterial species [8]. Once taken up, the iron is released from the host protein and becomes available to the bacterium.

As mentioned previously, bacteria can also acquire iron in an indirect fashion by synthesizing and secreting iron-chelating molecules called siderophores and hemophores. Siderophores are small (<1,000 Da) peptide-based molecules with an extremely high affinity for Fe(III) [8]. Upon binding Fe(III), siderophores return to the bacterial cell where they are recognized by surface proteins and internalized. Iron may be released from siderophores by reduction of Fe(III) to Fe(II) (siderophores have a much lower affinity for Fe(II)) or by breaking down the siderophores and releasing the iron. Hemophores make up the second class of secreted iron-binding molecules and are found only in Gram negative bacteria [8]. Hemophores can bind heme-hemopexin, heme-hemoglobin, or free heme, but regardless of the heme source, the heme-hemophore complex is bound by a cell surface receptor and internalized.

Once inside the cell, the iron acquired from the different sources is incorporated into bacterial proteins. In times of iron excess, bacteria can utilize the iron storage proteins bacterioferritin and Dps (similar to ferritin) that sequester iron safely. Bacterial iron uptake systems are both positively and negatively regulated at the gene level. For reviews on this subject, refer to Wandersman and Delepelaire [8] and Andrews *et al.* [9].

1.3 Yeast Iron Metabolism

Yeast is an excellent model organism to study iron homeostasis as many proteins involved in this process appear to be conserved between yeast and humans. Two mechanisms for iron uptake have been described for yeast: siderophore iron uptake and

reductase-dependent iron uptake. The use of siderophores (described in Section 1.2) to acquire iron is interesting as yeast do not necessarily have to synthesize the siderophore themselves [10]. In fact, *Saccharomyces cerevisiae* lack any biosynthetic pathway for siderophores and are able to scavenge siderophores produced by other micro-organisms such as fungi or bacteria. Yeast express permease proteins on their cell surfaces for various siderophores making siderophore scavenging an effective method of iron acquisition [10]. The second uptake mechanism relies on the reduction of Fe(III) to Fe(II) prior to uptake [10]. Fe(III) is reduced by a membrane reductase protein (specifically, Fre1p or Fre2p). Subsequent to this reduction step, the Fe(II) can enter the cell in two ways. First, the Fe(II) can enter the cell directly via a divalent metal ion transport protein similar to divalent metal transporter-1 (DMT-1) in humans or via the low affinity Fe(II) transporter Fet4p. Second, the Fe(II) is reoxidized to Fe(III) by the membrane-bound multicopper ferroxidase Fet3p prior to being taken up by the Fe(III) permease Ftr1p [10]. Fet3p and Ftr1p act in concert for both the incorporation of copper into the Fet3p and for the membrane localization of both proteins; indeed, a recent study demonstrated that Fet3p and Ftr1p physically interact with each other [11]. In yeast, iron homeostasis is regulated by the transcription factor Aft1p, and targets of its transcriptional activation are genes that encode proteins necessary for iron uptake, including *Fet3* and *Ftr1* [10]. Unlike bacteria and humans, *S. cerevisiae* do not possess the iron storage protein ferritin; instead, iron storage occurs in vacuoles [12]. Much of the iron needed by yeast is incorporated into mitochondrial iron-sulfur proteins and cytochromes, such that mitochondria represent the central location for the synthesis of iron-containing molecules destined for incorporation into cellular proteins [12]. The mechanisms

for iron transport to and from the mitochondria are unknown, but it is likely that an iron chaperone, similar to those described for copper [13], exists to fill this role.

1.4 Human Iron Metabolism

Dietary iron absorption occurs in the proximal small intestine by specialized epithelial cells called duodenal enterocytes. Hemoglobin found in dietary meat contains iron complexed to heme and in the developed world, it has been estimated that more than half of all absorbed iron is from heme. However, in the rest of the world and especially in third world countries, most dietary iron is obtained as Fe(III) from plant sources. Pharmaceutical iron supplements supply iron in the Fe(II) state and this may be another source of iron in some diets (reviewed in [14]). To date, three pathways for iron uptake are recognized, two of which are shown in Figure 1.1.

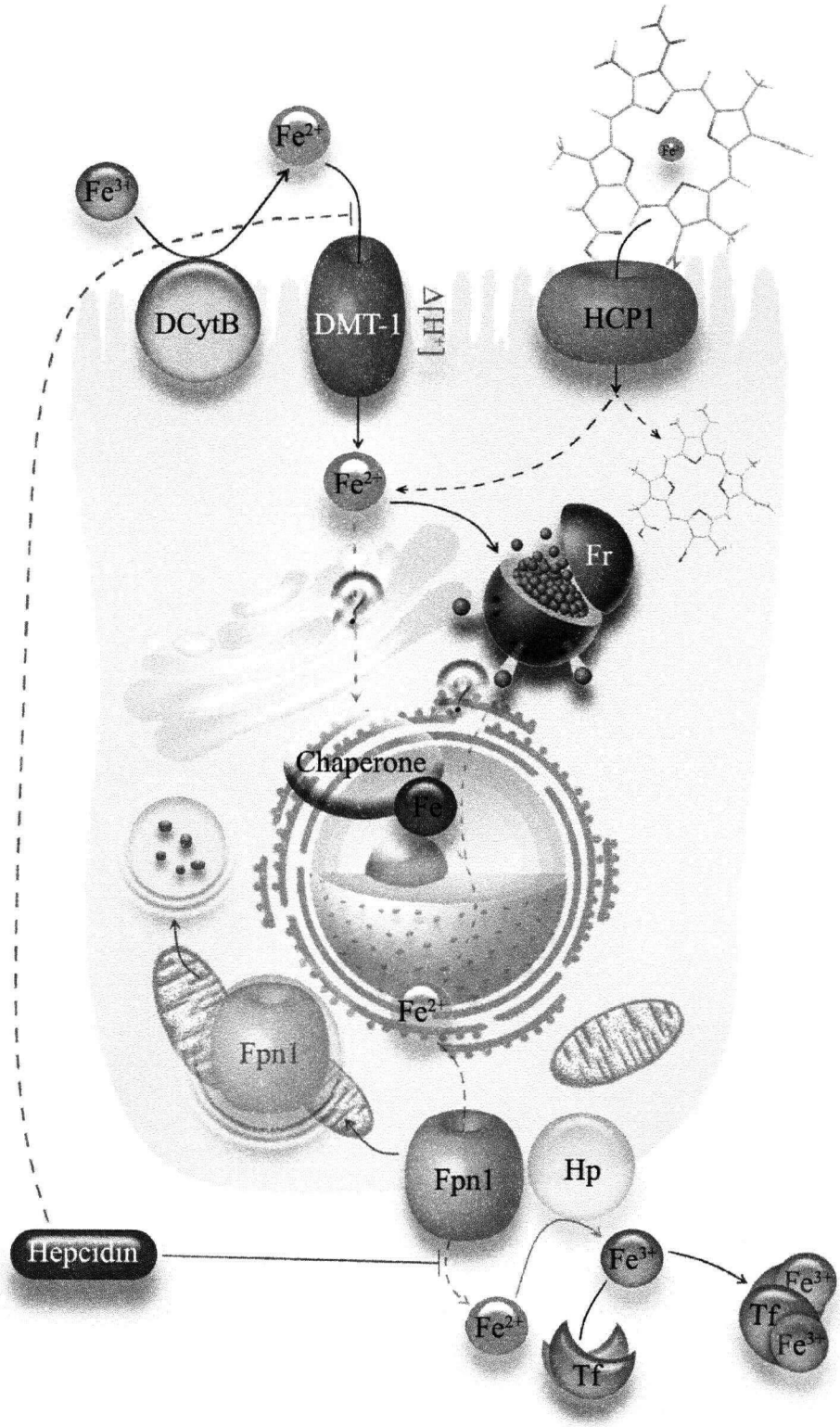

Figure 1.1 Proposed iron homeostasis in an intestinal enterocyte cell. Proteins are shown with abbreviated names, ferritin is designated Fr (this figure is courtesy of Ann Wong). See text for details.

The mechanisms for inorganic iron uptake allow for both Fe(III) and Fe(II) to be transported into the enterocyte. Conrad and Umbreit [4] have shown evidence for an integrin-mobilferrin pathway in which Fe(III) is chelated by mucins in the lumen of the small intestine and this complex is subsequently taken up into the enterocyte by β_3 integrin and mobilferrin; however, this pathway is not well characterized and as a result, has been omitted from Figure 1.1. McKie *et al.* have demonstrated that an intestinal ferrireductase, DCytB, reduces Fe(III) to Fe(II) [15] thus allowing the Fe(II) to be transported into the cell by the apical transmembrane protein DMT-1 [16-18]. As DMT-1 is a transporter of divalent metal ions, Fe(II) from dietary iron supplements is readily transported into the enterocyte. If more iron is absorbed into the enterocyte than required, the excess iron will be stored in the iron storage protein ferritin until needed or until the enterocyte dies at which time the stored iron will be lost to the stool.

Until very recently, the uptake mechanism for heme iron was unknown, but seminal studies by Shayeghi and colleagues have identified the mouse intestinal heme carrier protein 1 (HCP1) [19]. HCP1 is a transmembrane protein that is expressed in the duodenum and transports the intact iron porphyrin across the apical enterocyte membrane. Once the iron porphyrin is inside the enterocyte, the heme is degraded and the iron is released allowing it to join the low molecular weight iron pool and be exported from the cell (*vide infra*).

Absorbed dietary iron that is required to maintain body iron homeostasis must be transported across the enterocyte, presumably by a currently unidentified iron chaperone, and subsequently exported out of the cell and into the circulation. The integral membrane protein ferroportin 1 (Fpn1) is on the basolateral enterocyte membrane and exports ferrous iron from the intestine [20, 21]. Once in the blood plasma, the iron must be bound by the

plasma iron transport protein, apo transferrin (apo Tf). Transferrin (Tf) does not bind Fe(II); hence, a ferroxidase activity on the basolateral membrane surface, attributed to hephaestin (Hp), is believed to be essential for the transfer of iron from the gut mucosa to blood (for a review, see Aisen *et al.*, 2001 [3]).

The Fe(III) bound by Tf is transported throughout the body [22]. About 85% of Tf-bound iron is delivered to reticulocytes to be incorporated into hemoglobin. The remaining iron can be incorporated into other iron-containing proteins such as the cytochromes and myoglobin. Two atoms of iron can be bound per molecule of Tf and Tf has a high affinity for only Fe(III), not Fe(II) [22]. Iron-loaded Tf binds to the Tf receptor (TfR) that is ubiquitously present on the plasma membranes of all cells, and by receptor-mediated endocytosis, the Tf is internalized [23]. Once inside the cell, the Tf-TfR complex is found in an endosome that subsequently undergoes a lowering of the pH via proton pumps thereby releasing iron from the Tf. Seminal work by Ohgami and colleagues [24] describes the discovery of Steap3 – an endosomal ferrireductase protein that reduces Tf-released Fe(III) to Fe(II). This reduction step is necessary for endosomal Fe(II) export through DMT-1. Following release of Fe(II) from the endosome into the cellular milieu, both the Tf and the TfR are redeposited on the outside of the cell to perform further cycles of iron binding and delivery (see [3, 22, 23, 25] for reviews).

The regulation of iron absorption was poorly understood until the recent discovery of hepcidin [26]. This 25 amino acid antimicrobial peptide is expressed in the liver and is a negative regulator of iron absorption [27]. Hepcidin has been coined the "master iron regulatory hormone" [21]. One hypothesis regarding the mechanism by which hepcidin functions to regulate iron homeostasis was presented by Frazer and Anderson and involves

Tf, TfR1, and the hereditary hemochromatosis protein (HFE) [28]. Briefly, they proposed that when body iron stores are replete, there is sufficient diferric Tf to bind to TfR1; as a result, HFE binding to TfR1 is blocked. This leaves HFE free to signal for the upregulation of *hepcidin* expression, which ultimately decreases dietary iron absorption. When insufficient iron is being absorbed from the gut or when body iron demands exceed supply, less diferric Tf is available to bind TfR1. This facilitates an HFE-TfR1 interaction and consequently prevents the HFE-mediated upregulation of *hepcidin* expression. Hepcidin itself has been shown to bind to Fpn1 and result in internalization of Fpn1 thus decreasing iron efflux from the enterocyte [29]. However, others have found that hepcidin decreases the expression of DMT-1 thereby decreasing iron influx to the enterocyte [30]. Both mechanisms ultimately decrease body iron absorption and whether hepcidin regulates iron homeostasis by reducing iron influx or efflux (or both) remains to be determined. Senescent erythrocytes are phagocytosed by macrophages of the reticuloendothelial system allowing for the recycling of most of the body's iron [31]. As is evident from the complicated processes involved in iron uptake and homeostasis, regulation of iron levels is essential for survival. Numerous disorders of humans, such as Parkinson's disease or Alzheimer's disease [32], are associated with improper iron homeostasis.

1.5 Copper: Introduction to a Second Transition Metal

Similar to iron, copper is also an important biological transition metal. Copper is coordinated to proteins by specific amino acid side chains that act as ligands. By varying the amino acids that ligate the copper atom, distinct copper centres are produced. For the

purposes of this dissertation, three copper centres will be discussed; these are type 1 (T1), type 2 (T2), and type 3 (T3).

Proteins containing T1 copper atoms are referred to as "blue copper proteins". Each T1 copper is ligated by two histidyl residues, one cysteinyl residue, and one methionyl residue, although the latter can also be a leucyl residue. The His and Cys ligands coordinate the copper atom in a trigonal equatorial fashion, while the Met (or Leu) residue is in an axial position with respect to the metal. This axial position of the Met results in a longer bond length between the ligand and the metal and thus, a weaker interaction. Due to the highly covalent nature of the Cys(S)-copper bond, ligand to metal charge transfer occurs giving proteins containing T1 copper sites their intense absorption in the visible region of the spectrum (λ_{max} ~600 nm, ε ~5,000 M^{-1} cm^{-1}) and characteristic blue colour (reviewed by Solomon and Lowery [33]).

The T2 and T3 copper sites behave as a functional unit comprising one T2 copper atom and two binuclear coupled T3 copper atoms. This trio of copper atoms is referred to as a trinuclear copper cluster. Spectroscopic properties of the trinuclear cluster include an electron paramagnetic resonance profile similar to typical copper complexes (from the T2 copper atom) and optical absorbance at ~330 nm (ε ~5,000 M^{-1} cm^{-1}, from the T3 copper atoms) [33]. The T2 copper atom is ligated by two histidyl residues and a water molecule in a square planar geometry with the open coordination position directed towards the binuclear T3 copper atoms. The T3 copper atoms are four-coordinate, each ligated by three histidyl residues and bridged by an oxygen molecule (in the form of hydroxide) to the other T3 copper atom. The geometry of each of these T3 copper centres is described as trigonal bipyramidal with an empty equatorial coordination site directed towards the open

coordination position of the T2 copper site [34]. The presence of all three types of copper sites (T1, T2, and T3) in a single protein is characteristic of a particular group of enzymes called multicopper oxidases (MCOs).

1.6 Multicopper Oxidases

MCOs have the ability to couple the oxidation of substrate to the four electron reduction of dioxygen to two water molecules. These enzymes are found in a variety of organisms from bacteria to humans. Reducing substrates for the different MCOs are diverse and include phenolic compounds (laccase), L-ascorbic acid (ascorbate oxidase), and inorganic metal ions such as Fe(II) (CueO, Fet3p, Cp) [35] (Figure 1.2).

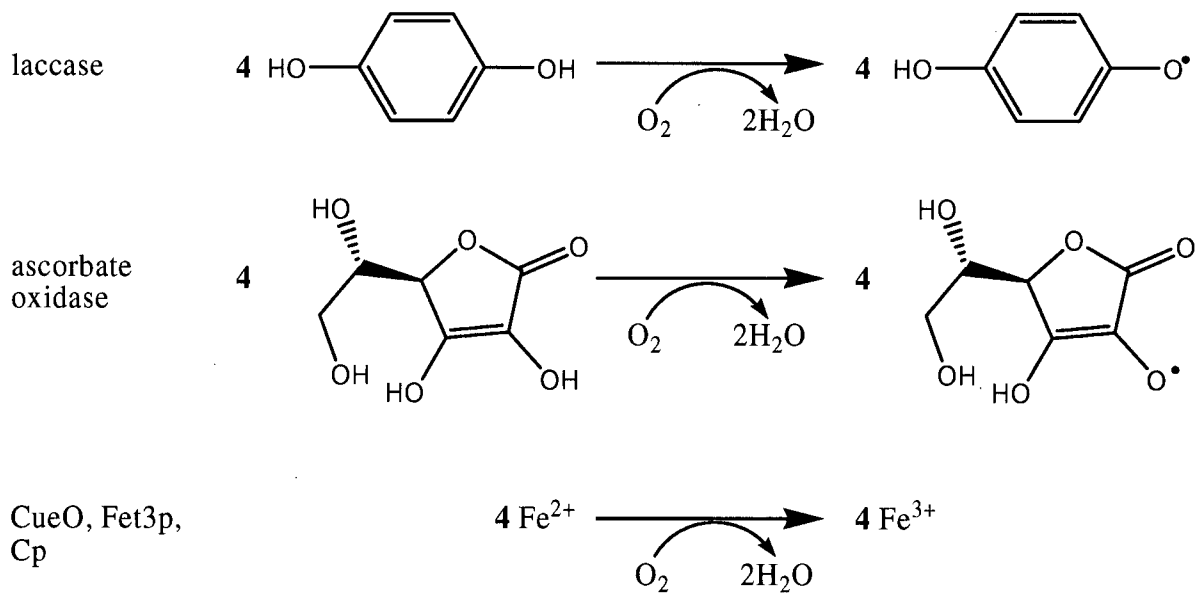

Figure 1.2 Reactions mediated by the MCOs using a variety of reducing substrates.

The simplest MCOs (laccase, Fet3p, and CueO) contain four integral copper atoms – one T1 copper atom and the trinuclear cluster. These four copper atoms are thought to be the minimum number required for a MCO to be enzymatically active. Human Cp is one of the largest and best characterized MCOs and binds six integral copper atoms distributed throughout three T1 sites and the trinuclear cluster [36] (Figure 1.3).

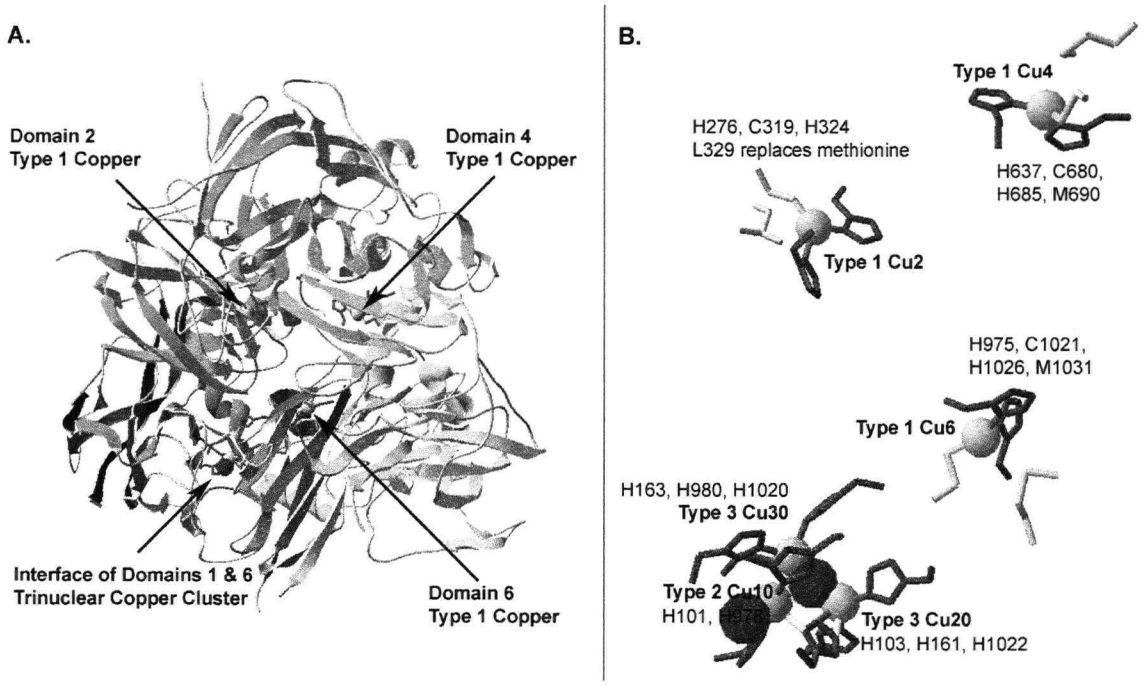

Figure 1.3 The structure of human Cp. A. Ribbon diagram of Cp showing the six domains of the protein as well as the locations of the integral copper atoms and their ligands. **B.** The six integral copper atoms of Cp and their amino acid ligands. Copper atoms are in grey spheres, while oxygen atoms are red spheres. These models were generated from the published coordinates for human Cp [36] using the program Swiss-Pdb Viewer, version 3.7 (available online at http://www.expasy.org/spdbv/).

To date, only three MCOs have shown the ability to utilize Fe(II) as a reducing substrate: CueO [37], Fet3p [38], and Cp [39] (Table 1.1). Although CueO has been shown

to oxidize iron *in vitro*, it is not known if Fe(II) truly represents a substrate *in vivo* [37, 40, 41].

Table 1.1 MCOs known to use inorganic Fe(II) as a reducing substrate.

Protein	Organism	Number of Amino Acids	Total Number of Integral Copper Atoms	Ref.
CueO	*Escherichia coli*	516	4 (1 x T1 & T2/T3 cluster)	[37]
Fet3p	*Saccharomyces cerevisiae*	636	4 (1 x T1 & T2/T3 cluster)	[42]
Cp	*Homo sapiens*	1065	6 (3 x T1 & T2/T3 cluster)	[36]

1.7 Enzymatic Ferroxidase Activity

MCOs that utilize Fe(II) as substrate (hereinafter referred to as ferroxidases) prevent formation of the highly oxidizing hydroxyl radical by binding O_2 in its partially reduced states and releasing only water. Extensive work on the potential mechanisms by which O_2 may be reduced to water and the electron transfer pathways to facilitate this reduction has been completed by Edward Solomon's group and the reader is directed to a number of his publications [34, 35, 43]. Findings from the most recent study describing the reduction of O_2 to H_2O are depicted in Figure 1.4 and described [44]. Fe(II) binds to the fully oxidized ferroxidase near a T1 copper site (not shown). Electrons are transferred sequentially from four Fe(II) to the T1 copper atom and ultimately to the trinuclear copper cluster (not shown); all copper sites in the ferroxidase, including the T1 copper atom (not shown), are reduced (Figure 1.4, A) and four Fe(II) are oxidized to four Fe(III) (not shown). Dioxygen binds to

the trinuclear cluster and is partially reduced by electrons from the T3 binuclear copper atoms (Figure 1.4, B). Another reducing equivalent is donated to the trinuclear cluster, presumably from the T1 copper atom; however, the O_2 molecule stays intact (Figure 1.4, C). In the last step, reductive cleavage of the O-O bond is seen and $2H_2O$ molecules are released from the active site (Figure 1.4, D). All copper sites are again oxidized and ready to accept electrons from the Fe(II) substrate and continue the cycle (Figure 1.4, A).

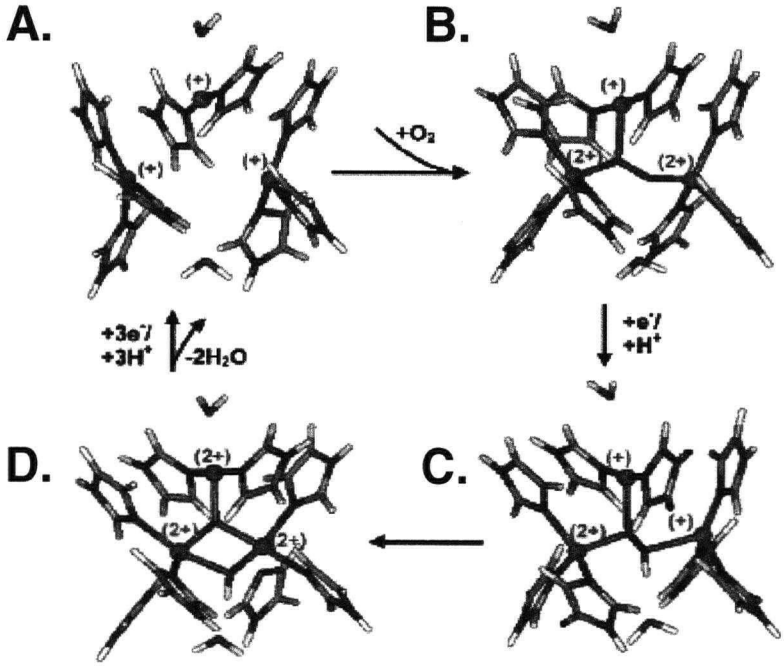

Figure 1.4 Predicted mechanism for the reduction of O_2 to H_2O in the ferroxidases. This figure was adapted from [44], the T1 copper site is not shown in the model.

As alluded to previously, ferroxidases have two active sites (one for Fe(II) oxidation, the other for O_2 reduction) and function via a ping-pong mechanism [45, 46]:

$$4Fe(II) + 4Cu(II) \rightarrow 4Fe(III) + 4Cu(I)$$

$$4H^{+} + O_2 + 4Cu(I) \rightarrow 2H_2O + 4Cu(II)$$

Reduction potentials of electron donors and acceptors determine the direction of electron flow in the ferroxidases. The reduction potentials increase from the initial electron donors (Fe(II) complexes [~300 mV depending on the ligand]) to the T1 copper site(s) (~400-500 mV for catalytically active sites) to the ultimate electron acceptor, O_2 (820 mV) [47]. The reduction potentials for the T1 (blue) copper sites of Cp and Fet3p as well as the amino acid ligands coordinating the T1 sites in all known ferroxidases are shown (Table 1.2). It is of significance that the T1 copper site in domain 2 of human Cp has a very high reduction potential. It was proposed by Machonkin *et al.* [46] that the copper in this T1 site is permanently reduced and cannot participate in the oxidation of substrate. Accordingly, this site is considered catalytically inactive leaving only two functional T1 sites in human Cp. The high reduction potential has been attributed to stabilization of the Cu(I) state by the absence of the axial methionyl ligand (replaced with a leucyl residue that does not coordinate the copper, refer to Figure 1.3). However, absence of this axial ligand, although a contributor to an increased reduction potential, cannot be the only factor. This is demonstrated by the T1 copper site of Fet3p in which the methionyl ligand is also absent. The reduction potential for this site in Fet3p is similar to those found in domains 4 and 6 of human Cp. It has been suggested that the protein matrix itself can aid in tuning the potential of the T1 copper site(s) to the appropriate value(s) [48].

Table 1.2 Reduction potentials (mV *vs.* normal hydrogen electrode (NHE)) and amino acid ligands of the T1 copper sites found in the ferroxidases.

Species	Protein	$E°$ (pH 7) (mV *vs.* NHE)	T1 Ligands	Ref.
H. sapiens	Cp (domain 2)	≥ 1,000	2 His 1 Cys 1 Leu	[46]
H. sapiens	Cp (domain 4)	448	2 His 1 Cys 1 Met	[43]
H. sapiens	Cp (domain 6)	491	2 His 1 Cys 1 Met	[43]
S. cerevisiae	Fet3p	427	2 His 1 Cys 1 Leu	[49]
E. coli	CueO	*nd*[1]	2 His 1 Cys 1 Met	[40]

[1] *nd*: not determined

Enzymatic ferroxidase activity can be measured using Fe(II), in the form of ferrous ammonium sulfate hexahydrate, as substrate. Auto-oxidation of Fe(II) is significant during *in vitro* ferroxidase reactions, especially as the pH increases; thus, background ferroxidase rates of reaction mixtures containing no enzyme must be taken into account. There are two methods, continuous and discontinuous, for measuring the conversion of Fe(II) to Fe(III). The continuous method has been described by Bonomi *et al.* [50] and involves directly monitoring the production of Fe(III) via UV spectroscopy ($\Delta\varepsilon_{315} = 2200\ M^{-1}\ cm^{-1}$). The

discontinuous method relies on the properties of an Fe(II) chelator called 3-(2-pyridyl)-5,6-bis(4-sulfophenyl)-1,2,4-triazine (or ferrozine) (Figure 1.5). Ferrozine in solution is colorless, but the Fe(II)-ferrozine complex is a bright pink colour; thus, substrate depletion can be determined from the residual absorbance of the ferrozine-Fe(II) complex (ε_{562} = 27,900 M^{-1} cm^{-1}) [51]. Under the experimental conditions used for the discontinuous assay, Fe(II) conversion to Fe(III) is irreversible and Fe(III) does not inhibit the reaction so standard Michaelis-Menten analysis is appropriate.

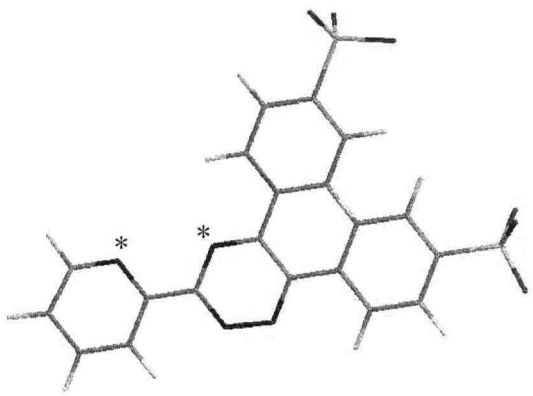

Figure 1.5 Structure of ferrozine. Ferrozine is colourless in solution until Fe(II) is coordinated by nitrogen atoms (indicated with *) in a bidentate fashion. Colour legend for atoms: carbons are grey, hydrogens are white, sulfurs are yellow, oxygens are red, and nitrogens are blue.

1.8 Hephaestin

An early candidate for the ferroxidase activity in intestinal iron absorption was the multicopper oxidase ceruloplasmin (Cp). However, despite Cp possessing ferroxidase activity, there is no evidence to support a role for Cp as the intestinal ferroxidase as patients with aceruloplasminemia do not have impaired dietary iron absorption [52]. An alternative

candidate for this ferroxidase activity arose from two discoveries. First, a mouse mutant was described in 1962 that exhibited an X-linked, recessive hypochromic, microcytic anemia. The gene responsible for this disorder was called *sex-linked anemia* or *sla [53]*. Subsequent studies showed that the anemia could be corrected by intraperitoneal delivery of Fe(II) but not by ingested iron [54] and that the *sla* mutation involved a defect in the transport of iron from the enterocyte to the blood plasma [55, 56]. The second discovery arose from genome sequencing projects in which a Cp homologue was identified on the mouse [57] and human [58] X chromosomes. The predicted polypeptide encoded by the candidate gene shared 50% sequence identity with Cp and was called Hp after Hephaestus, the Greek god of metallurgy [57].

From the mRNA sequence (NCBI accession number AJ296162), human Hp was predicted to consist of 1158 amino acids (NCBI accession number NP_620074) and have a calculated mass of 130,000 Da without glycosylation and ~155,000 Da with glycosylation [58, 59]. Syed *et al.* [58] have used the sequence identity between Cp and Hp to construct a hypothetical model of the structure of Hp. Based on this model, Hp is predicted to have 6 domains forming a pseudo-threefold axis. However, unlike Cp (a soluble plasma protein), Hp is predicted to have an extra 86 amino acids at the C-terminus that include a transmembrane domain and a short cytosolic tail. All residues (with the exception of the axial T1 ligand in domain 2) involved in Types 1, 2, and 3 copper binding as well as cysteinyl residues involved in disulfide bond formation in Cp are conserved in Hp (Appendix A); thus, Hp could potentially bind up to 6 copper atoms. Based on computer modeling studies, it is predicted that the mononuclear T1 copper atoms are located in domains 2, 4, and 6 with a trinuclear T2/T3 cluster at the interface of domains 1 and 6 [58].

Evidence supporting a role for Hp as the cause of the murine hypochromic, microcytic anemia came from the identification of a 582 nucleotide deletion in the *hp* mRNA in the *sla* mouse [57]. Subsequently, Frazer *et al.* [59] prepared an anti-peptide antibody to mouse Hp, and others have used this antibody to show that mouse enterocyte membranes contain a protein with ferroxidase activity that comigrates with Hp during polyacrylamide gel electrophoresis (PAGE) [60].

Details of the Hp catalyzed oxidation of Fe(II) to Fe(III) *in vivo* and subsequent transfer of Fe(III) to apo Tf are presently unknown. A recent study by Kuo *et al.* [61] showed that Hp is present not only on the basolateral membrane of enterocytes, but also in an apical supranuclear position and in the recycling endosome compartment. The presence of Hp on the basolateral membrane is expected if Hp is to facilitate iron export from the gut in association with Fpn1. However, the presence of Hp in the recycling endosome and in apical supranuclear compartments is harder to explain. It has been proposed that Hp cycles between the basolateral membrane (where it may interact with Fpn1) and the recycling endosome [2, 61]. The pool of Hp that exists in the apical supranuclear compartment may have a unique function that is presently unknown [61].

1.8.1 Tissue Specific Expression of Hephaestin

Consistent with its role as an intestinal ferroxidase, Hp is expressed at the highest level in the small intestine [57]. However, Hp is also expressed in a variety of other tissues including the brain, kidney, lung, and retinal pigment epithelium [57, 58, 62]. The function of Hp is these tissues is unknown with the exception of the retinal pigment epithelium where it has been shown that both Cp and Hp are necessary to prevent iron overloading and

subsequent retinal deterioration. It is hypothesized that these ferroxidases act to export iron out of the retinal pigment epithelium cells [62].

1.8.2 Recombinant Expression of Hephaestin

At the beginning of my thesis studies, recombinant expression of a secreted, soluble form of Hp amenable to enzymatic and spectroscopic investigation had not been reported. Li and colleagues [63] attempted expression of mouse Hp in yeast, but could not facilitate secretion of the protein, even with removal of the transmembrane domain. The expression of a recombinant Hp-green fluorescent protein fusion protein has been reported in a poster abstract to a Biochemical Society Meeting held in April 2002 (http://www.biochemistry.org/meetings/postertoc/SA2/default.htm), but the details of this study have not yet been published in a peer-reviewed paper.

1.8.3 Recombinant Expression of the Ferroxidases Ceruloplasmin, Fet3p, and CueO

Recombinant human Cp has been expressed, but the yields have been low. Bielli *et al.* [64] expressed human Cp in the yeast *Pichia pastoris*. Purification of recombinant human Cp was complicated by the need to separate it from the endogenous *P. pastoris* Fet3p. Following purification, the yield of Cp was ~1.2 mg/L of culture medium. Like the human plasma-derived protein, the recombinant Cp was highly susceptible to proteolysis; however mutation of three residues (R481, R701, and K887) rendered recombinant human Cp stable to proteolysis. Spectroscopic studies indicated that recombinant human Cp behaved similarly to plasma-derived human Cp. Mauk and colleagues [51] have also expressed

human Cp in human embryonic kidney (HEK) 293 cells and characterized several mutant forms that had reduced ferroxidase activity.

Similar to Hp, Fet3p has a C-terminal transmembrane domain. Bonaccorsi di Patti *et al.* [65] released endogenous Fet3p from *P. pastoris* cell membranes by limited proteolysis. The purified, soluble Fet3p contained ferroxidase activity and spectroscopic characteristics consistent with other ferroxidases. Hassett and colleagues expressed recombinant Fet3p lacking the transmembrane region in *S. cerevisiae* that was secreted into the growth medium as a soluble protein. Fet3p was expressed at a concentration of 5 mg/L, and at a concentration of 7.7 mg/mL had a blue color characteristic of multicopper oxidases [66].

The multicopper oxidase required for copper homeostasis in *E. coli* is CueO. Recently, CueO was overexpressed in bacteria, its crystal structure determined, and its electron transfer kinetics investigated [40]. A subsequent study reported expression levels of 1 mg of CueO per litre of culture medium [67].

1.9 Statement of Hypotheses

The hypotheses in this dissertation are threefold:

1. Based on the sequence similarity with the human Cp polypeptide (Appendix A), a recombinant form of human Hp lacking the transmembrane domain can be expressed.
2. Based on the sequence similarity with the human Cp polypeptide, recombinant human Hp will bind copper and have ferroxidase activity.
3. Fe(III) generated from the ferroxidase activity of recombinant human Hp can be loaded onto apo Tf.

1.10 Objectives

The family of ferroxidases is growing and each new member has a unique characteristic that has not been observed in previous members of the family. For instance, Fet3p possesses a C-terminal membrane tether, Hp possesses an axial methionyl ligand in each of the putative T1 copper sites, and CueO possesses a methionine-rich α-helix that is thought to be involved in copper binding. Hp is only the second vertebrate ferroxidase to be discovered and there have been virtually no studies that attempt to characterize the physical, spectroscopic, and enzymatic properties of purified human Hp. Because of the proposed role of Hp in iron metabolism, four questions were addressed in this study:

1. Can human Hp lacking the C-terminal transmembrane domain be expressed in a mammalian cell line?
2. What are the physical and spectroscopic characteristics of recombinant human Hp?
3. Does recombinant human Hp possess oxidase activity that is comparable to the activities of Cp and Fet3p?
4. Can the ferroxidase activity of recombinant human Hp be used to load apo Tf with Fe(III)?

Chapter 2. Materials and Methods

2.1 Materials

HEK 293 cells, cell culture medium, and anti-bovine rhodopsin monoclonal antibody (anti-1D4) Sepharose 2B were kindly provided by Dr. Robert Molday, Department of Biochemistry and Molecular Biology, University of British Columbia, Canada. Coupling of the anti-1D4 monoclonal antibody to CNBr-activated Sepharose 4B (GE Healthcare, Piscataway, NJ) was carried out at a concentration of 2 mg/mL according to the supplier's instructions (GE Healthcare). Large unilamellar vesicles (LUVs) composed of equimolar amounts of N,N-dioleyl-N,N-dimethylammonium chloride:dioleoylphosphatidylethanolamine (DODAC:DOPE) were kindly provided by Dr. Pieter Cullis (Department of Biochemistry and Molecular Biology, University of British Columbia). Expand High Fidelity *Taq* polymerase was obtained from Roche (Mississauga, ON). Ferrous ammonium sulfate hexahydrate (ReagentPlus grade) was obtained from Sigma-Aldrich (Oakville, ON). Peptide synthesis was performed by the Nucleic Acid Protein Service (NAPS) at the University of British Columbia, and oligonucleotide synthesis was performed by NAPS and Operon Biotechnologies (Huntsville, AL). DNA restriction- and modification enzymes were from New England Biolabs (Beverly, MA). Tissue culture multi-well plates were supplied by BD Falcon (Oakville, ON), Corning expanded surface roller bottles and 100 mm diameter Petri dishes were from Fisher Scientific (Ottawa, ON). All sodium dodecyl sulfate-polyacrylamide gel electrophoresis (SDS-PAGE), Western blotting, polymerase chain reaction (PCR), and cloning steps were performed using established protocols [68]. Unless otherwise noted, HEK 293 cells and baby hamster kidney

(BHK) cells were grown at 37 °C in a 5% CO_2 environment. Amino-terminal sequence analysis and electrospray ionization/matrix assisted laser desorption ionization time-of-flight mass spectrometric (MALDI TOF MS) analyses were carried out by the Laboratory of Molecular Biophysics Proteomics Core Facility, University of British Columbia. Amino acid analysis (AAA) was performed at the Protein Chemistry Laboratory, Texas A&M University (College Station, TX).

2.2 Isolation of Total RNA from Human Duodenum and First Strand Synthesis

A sample of human duodenal tissue from a brain dead organ donor was kindly provided by Dr. Mark Meloche (Department of Surgery, University of British Columbia, Canada). Institutional approval for the use of human material in research was obtained by Dr. Meloche as part of the transplantation program. Total RNA was isolated from the duodenal tissue using a TRIzol kit (Invitrogen, Burlington, ON) according to the supplier's recommendations. The RNA was stored at -70 °C until use.

The tissue specific expression of human Hp was analyzed using RNA samples from 3 sources: duodenum (described previously), brain, and an endothelial cell line. The sample of human brain (central cortex) mRNA was obtained from the laboratory of Dr. Michael Hayden (Department of Medical Genetics, University of British Columbia, Canada) in 1986. The sample was stored at -70 °C until use. The human endothelial cell mRNA was obtained from Immuno AG (Vienna, Austria) in 1989. The sample was stored at -70 °C until use. First strand cDNA synthesis was performed using 8 µg RNA, Superscript II Reverse Transcriptase (Invitrogen), and both $pd(N)_6$ random hexamers and $(dT)_{12\text{-}18}$ oligonucleotides (GE Healthcare) as primers according to supplier's suggestions. PCR primer sequences for

human Hp were provided by the HUGE Protein Database (http://www.kazusa.or.jp/huge/gfpage/KIAA0698/) and were designated KIAA_F and KIAA_R (Table 2.1).

Table 2.1 Oligonucleotides used to amplify the human Hp coding region (shown 5'→3'). F denotes a forward primer, R denotes a reverse primer.

KIAA_F	TGAAGGTAGGCTGAGTATTGG
KIAA_R	CTCAACATTCCTTTCAGTGCC
Fragment 1F	CTGGACACGTAGAAAGCCCCTTTGTTC
Fragment 1R	ATTGCATGCATCCTATTGCTCTCCTGA
Fragment 2F	TGGGCCACTGAAAGCTGATGAC
Fragment 2R	CCCAGGATTCCAAGATGCCTATCT
Fragment 3F	GCTGAGATGGTGCCCTGGGAACC
Fragment 3R	TGTCAGGCTGCATGATGGCCA
Fragment 4F	CCATAAGAGACACAAATTCTGGCCTGGTG
Fragment 4R	CTCTGGGATGTTCCACTGATAAGTGACCAC
Fragment 5F	CATGCTCATGGAGTGCTAGAATCTACT
Fragment 5R	TACAGATGTGCTTCCTGAGGATATCTC

2.3 Cloning the Hephaestin cDNA

Based on similarity of the Cp and Hp genes, the entire Hp cDNA was predicted to be 4,854 bp in length [58]. Five pairs of PCR primers were designed (Table 2.1) and used to amplify the Hp coding region from the cDNA in 5 overlapping fragments, each fragment containing unique restriction sites (from 5'→3': *Xma*I, *Sac*I, *Eco*RI, and *Blp*I) (Figure 2.1). Individual PCR products were purified using the QIAquick PCR Purification kit (Qiagen, Mississauga, ON), cloned in the pBluescriptII SK$^-$ (pBSSK$^-$) vector (Stratagene, La Jolla, CA), and propagated in DH5α *E. coli*. Plasmid DNA was purified using a QIAprep spin miniprep kit (Qiagen). Following subsequent restriction digests and ligations, the entire Hp coding region was assembled. These constructs, and all constructs described hereinafter,

were verified by automated DNA sequence analysis using the BigDye Terminator kit and an ABI 3700 DNA sequencer (Applied Biosystems, Streetsville, ON).

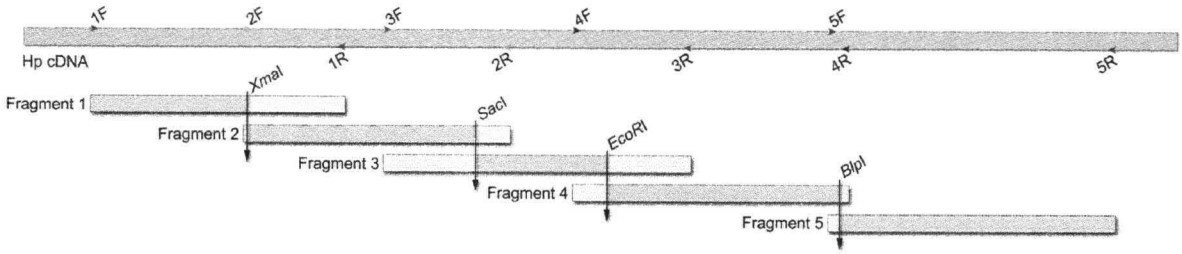

Figure 2.1 PCR amplification of Hp in five overlapping fragments. The aqua bar represents Hp cDNA. Primer pairs are indicated by arrow heads and are labeled according to Table 2.1. PCR fragments are shown by grey and white bars, restriction enzyme cut sites are shown by a black arrow. Following digestion of the fragments with the appropriate restriction enzyme, the grey fragments were ligated to reassemble the Hp coding region.

2.4 DNA Manipulation for Transient Expression in HEK 293 Cells

To produce Hp cDNA that would allow the transient expression and subsequent detection via Western blotting, three genetic engineering steps were completed: (i) the coding region for the putative C-terminal transmembrane region and for residues upstream of the transmembrane region that are not conserved in Cp was removed by truncating Hp at amino acid Ser1070 (all amino acid numbering for human Hp is according to NCBI Accession NP_620074); (ii) a Factor Xa (FXa) recognition sequence IEGR was introduced; and (iii) an immunogenic human c-Myc epitope [69] was introduced. The 3' end of the Hp-Myc construct is shown in Sequence 2.1 (Hp amino acid residues are denoted with superscript numbers, the reading frame is indicated by spaces, and the stop codon is shown with an asterisk):

```
     L1069 S1070  I   E   G   R   E   Q   K   L   I   S   E   E   D   L
5′ C TTA AGC ATC GAG GGA AGG GAG CAG AAA CTC ATC TCT GAA GAG GAT CTG
3′ G AAT TCG TAG CTC CCT TCC CTC GTC TTT GAG TAG AGA CTT CTC CTA GAC

 *
TAA 3′ (sense)
ATT 5′ (antisense)
```

Sequence 2.1 3' end of the Hp-Myc construct.

The Hp-Myc construct was excised from the pBSSK$^-$ vector via 5' and 3' *Hin*dIII and *Not*I restriction sites, ligated into the *Hin*dIII and *Not*I digested pcDNA3 vector (Invitrogen), and propagated in *E. coli* strain DH5α.

2.5 Transient Expression and Western Blotting of Hephaestin from HEK 293 Cells

For transfection of mammalian cells, plasmid DNA was purified from DH5α *E. coli* with the QIAprep spin miniprep kit. The Hp pcDNA3 expression vector DNA (24μg) or 24 μg of the pcDNA3 vector as a negative control was used to transfect the HEK 293 cells by the calcium phosphate co-precipitation method [70]. Forty-eight hrs following transfection, the conditioned medium and cell lysates were prepared for Western blotting. To prepare the cell lysates, transfected HEK 293 cells were scraped from the culture dish, washed once with phosphate buffered saline (PBS), and added drop wise to PBS containing 2% Triton X-100 while mixing on a vortex mixer. Western blots were performed after SDS-PAGE on a 10% gel and transfer to a polyvinylidene fluoride (PVDF) membrane in transfer buffer (25 mM Tris, pH 8.3, 192 mM glycine, 0.1% SDS, 10% methanol) for 2 hrs. The membrane was blocked in 1% skim milk powder in Tris buffered saline containing 0.05% Tween-20 (TBST), incubated with an anti-Myc antibody (1:200, Sigma-Aldrich) in TBST and anti-

Mouse IgG (whole molecule)–alkaline phosphatase antibody produced in goat (1:15,000, Sigma-Aldrich) in TBST and developed using nitro-blue tetrazolium chloride/5-bromo-4-chloro-3'-indolyphosphate p-toluidine salt.

2.6 DNA Manipulation for Stable Expression BHK Cells

To produce secreted Hp, five genetic engineering steps were completed: (i) the coding region for the native Hp signal peptide was removed and replaced with the signal peptide and the first four residues of human Tf to ensure efficient removal of the signal peptide by signal peptidase and subsequent secretion from BHK cells; (ii) the coding region for the putative C-terminal transmembrane region was removed by truncating Hp at amino acid Ser1070; (iii) a FXa recognition sequence IEGR was introduced; (iv) the 1D4 epitope was introduced [71, 72]; and (v) *NotI* sites were incorporated into the 5' and 3' ends. The 5' and 3' ends of the Hp-1D4 construct are shown in Sequences 2.2 and 2.3 (Hp amino acid residues are denoted with superscript numbers, the reading frame is indicated by spaces, the *NotI* sites are underlined, and the stop codons are shown with asterisks):

```
                  M   R   L   A   V   G   A   L   L   V   C   A   V   L
5' GCGGCCGCACC ATG AGG CTC GCC GTG GGA GCC CTG CTG GTC TGC GCC GTC CTA
3' CGCCGGCGTGG TAC TCC GAG CGG CAC CCT CGG GAC GAC CAG ACG CGG CAG GAT

 G   L   C   L   A   V   P   D   K   A²⁴  T²⁵
GGG CTG TGT CTG GCT GTC CCT GAT AAA GCC ACT 3' (sense)
CCC GAC ACA GAC CGA CAG GGA CTA TTT CGG TGA 5' (antisense)
```

Sequence 2.2 5' end of the Hp-1D4 construct.

```
     L1069 S1070 I   E   G   R   T   E   T   S   Q   V   A   P
5' C TTA AGC ATC GAG GGA AGG ACA GAG ACC AGC CAA GTG GCG CCT
3' G AAT TCG TAG CTC CCT TCC TGT CTC TGG TCG GTT CAC CGC GGA

 A   *   *
GCC TGA TGA GCGGCCGC 3' (sense)
CGG ACT ACT CGCCGGCG 5' (antisense)
```

Sequence 2.3 3' end of the Hp-1D4 construct.

The Hp-1D4 construct was excised from the pBSSK$^-$ vector via the 5' and 3' *Not*I restriction sites, ligated into the *Not*I digested pNUT vector [73], and propagated in DH5α *E. coli*.

2.7 Stable Expression of Hephaestin in BHK Cells

For transfection, plasmid DNA was purified from *E. coli* strain DH5α with the QIAprep spin miniprep kit. BHK cells were grown to confluence in 6-well tissue culture plates in Dulbecco's modified Eagle medium-Ham F12 nutrient mixture (DMEM-F12) containing 5% newborn calf serum (NCS) (Invitrogen). Lipoplexes were formed by mixing 10 μg of plasmid DNA with 40 mM LUVs in 1% glucose in a total volume of 500 μL; these were incubated on ice for 20 min prior to use. Lipoplexes were added in a drop wise fashion directly to the cell medium that was bathing the cells. Cells were incubated for 24 hrs, at which time 0.44 mM methotrexate was added to the medium to begin selection. Methotrexate resistant colonies containing the pNUT plasmid were evident 10 days following selection.

2.8 Immunoprecipitation and Western Blotting of Hephaestin from BHK Cells

To screen for the highest expressing clones, an anti-1D4 immunoprecipitation (IP) and Western blot were performed on the conditioned medium from 10 clones. Anti-1D4 monoclonal antibody coupled to Sepharose 2B was used to immunoprecipitate recombinant Hp from 5 mL of conditioned medium from each clone growing in a T-25 flask. The IP reactions proceeded for 60 min at room temperature after which time the samples were washed three times with PBS at room temperature. Purified Hp was eluted from the anti-1D4 antibody by incubation with 60 μL of 2% SDS in PBS for 15 min at 37 °C. The eluants from each of the IP reactions were electrophoresed by 10% SDS-PAGE and transferred to a PVDF membrane in N-cyclohexyl-3-aminopropanesulfonic acid (CAPS) buffer for 2 hrs. The membrane was blocked with 1% skim milk powder, incubated with anti-1D4 (1:500) and anti-mouse/goat IgG-horse radish peroxidase conjugate (1:15,000, Sigma-Aldrich) and developed by using Enhanced Chemiluminescence (ECL). Cloned cell lines expressing Hp at relatively high levels were expanded into larger flasks for transfer into roller bottles. Cloned cell lines expressing low levels of Hp were frozen in a liquid nitrogen apparatus in 95% DMEM-F12-NCS-methotrexate medium/5% dimethylsulfoxide.

2.9 Purification of Secreted, Soluble Hephaestin from BHK Cells

BHK cells were grown in expanded surface roller bottles (1700 cm^2) at 37 °C in an ambient atmosphere. The culture medium (200 mL/bottle x 3 bottles) was collected every 3 days. The conditioned medium from the first collection contained DMEM-F12, 5% NCS, and methotrexate whereas subsequent collections contained DMEM-F12, 2% Ultroser G (serum replacement, BioSepra, Marlborough, MA), and 10 μM $Cu(II)SO_4$.

Hp was purified from 600 mL of culture medium within 24 hrs of collection. The medium was clarified by vacuum filtration through a 0.45 μm cellulose filter (Millipore, Nepean, ON). Due to the weak buffering capacity of the sodium bicarbonate that was present in the tissue culture medium, 1 M Tris-HCl, pH 7.4, was added to the medium to a final volume of 10 mM Tris-HCl. This buffered medium was passed through a CNBr-Activated Sepharose 4B anti-1D4 immunoaffinity column (bed volume of column: 10 mL; flow rate: 2.5 mL/min; temperature: 4 °C) that had been equilibrated with 10 mM Tris-HCl, pH 7.4 containing 150 mM NaCl. The column was washed with 20 bed volumes of the equilibration buffer. The bound protein was eluted at room temperature with 5x5 mL volumes of the equilibration buffer containing 0.2 mg/mL of the 1D4 peptide (N-acetylation-TETSQVAPA). All eluants were combined and 10% SDS-PAGE/Coomassie blue staining was used to establish that the Hp in this sample was >95% pure. For verification of the presence of recombinant Hp, Western blots were performed as described previously (Section 2.8). Purified Hp was treated with Endo-H and PNGase F glycosidases according to the supplier's recommendation (New England Biolabs), and the deglycosylated Hp was visualized by SDS-PAGE/Coomassie blue staining. Deglycosylation of Hp by PNGase F was also performed in the absence of SDS. Hp was treated with 3,000 U of the enzyme for 24 h at 37 °C and visualized as described previously. For long term storage, purified Hp was concentrated to 10-30 μg of protein/μL using Amicon Ultra-15 Centrifugal Filter Units (30,000 nominal molecular weight limit (NMWL)) and Amicon Ultrafree-0.5 Centrifugal Filter Units (50,000 NMWL) (Millipore) and snap-frozen in liquid nitrogen prior to storage at -70 °C.

2.10 Amino Acid Analysis and Edman Degradation for Amino Terminal Sequence Analysis of Hephaestin

Protein concentration was initially determined from quantitative AAA. To ensure sample purity, immunoaffinity purified Hp was subjected to gel filtration chromatography on a Superose 12 column (GE Healthcare) in 10 mM Tris, pH 7.4, 150 mM NaCl (flow rate: 0.5 mL/min, room temperature). Following chromatography, eluants containing Hp were analyzed by SDS-PAGE and exchanged into 100 mM NH_4OAc buffer, pH 5.0. A UV-visible spectrum of this sample was collected to obtain the A_{280} value. Two identical samples were prepared for duplicate analyses and lyophilized under vacuum in a Speed-Vac prior to shipping to Texas A&M University. The samples were subjected to vapour phase hydrolysis by 6 N HCl at 110 °C for 24 hrs under argon atmosphere in the presence of phenol. The experimental molar absorption coefficient for the absorbance at 280 nm was 215,000 M^{-1} cm^{-1} and this was used for subsequent protein concentration determinations. For Edman degradation and amino-terminal sequence analysis, purified Hp samples were separated by 10% SDS-PAGE and transferred to a PVDF membrane in CAPS buffer. The region of the membrane containing the Hp was excised, and used directly for the N-terminal sequence determination.

2.11 MALDI TOF and ICP Mass Spectrometry

MALDI TOF MS was performed with an Applied Biosystems Voyager DE-STR instrument. A sample of purified Hp (18 μM) was mixed 1:1 (v/v) with sinapinic acid and applied to the stainless steel MALDI target by the dried droplet technique. Analysis of copper content was performed by inductively coupled plasma mass spectrometry (ICP MS)

with a Perkin-Elmer, Sciex Elan 6000 instrument that was calibrated with the Instrument Calibration Standard 2 (SPEX Certiprep, Metuchen, NJ). Samples of recombinant Hp and copper-loaded human Tf (apo Tf from Sigma-Aldrich was copper-loaded according to Garratt *et al.* [74]) were prepared for analysis by dilution in 1% HNO_3 (Trace Metal Grade, Fisher Scientific), that was, in turn, prepared with glass-distilled water that had been polished with a Nanopure water purification system. A solution of the 1% HNO_3 prepared with this polished water was used as a blank. All samples were spiked with a selenium internal standard (Sigma-Aldrich) and values were normalized to this internal standard. Although copper was of primary interest in the ICP MS experiments, zinc levels were also determined in both samples. The specific isotopes that were analyzed were ^{63}Cu, ^{64}Zn, and ^{82}Se. The protein concentrations of the samples were determined from A_{280} measurements using the molar absorption coefficients of 215,000 M^{-1} cm^{-1} for recombinant Hp and 93,000 M^{-1} cm^{-1} for human Tf [75].

2.12 Copper Incorporation by Hephaestin

To reconstitute recombinant Hp with copper, sodium ascorbate was added to the protein (in 10 mM Tris, pH 7.4, 150 mM NaCl) to a final concentration of 1 mM and Cu(II)SO_4 was added in three aliquots to give a total of a 10-fold molar excess with respect to Hp concentration [42]. The visible absorbance attributed to the T1 copper atoms was monitored by collecting UV-visible spectra after each addition of copper to the sample.

2.13 UV-Visible Spectroscopic Analysis of Hephaestin

UV-visible absorbance spectra were recorded with a Varian Cary 4000 spectrophotometer (25 °C) and a sub-micro masked cell (path length: 10 mm). Unless otherwise indicated, recombinant Hp was dissolved in 10 mM Tris, pH 7.4 containing 150 mM NaCl, and all samples were clarified by centrifugation prior to obtaining spectra. To assess if the T1 copper atoms were fully oxidized, 50 μM recombinant Hp was treated with a 30-fold molar excess of hydrogen peroxide (Sigma-Aldrich) and spectra collected. To remove the hydrogen peroxide, the protein sample was exchanged into the starting buffer using an Amicon Ultrafree-0.5 Centrifugal Filter Units (50,000 NMWL). A 500-fold molar excess of sodium ascorbate (Sigma-Aldrich) was used to reduce the T1 copper atoms, spectra were again collected, and the sample was exchanged into starting buffer as described previously. This oxidation-reduction cycle was repeated.

2.14 Analysis of the Ferroxidase Activity of Hephaestin

Oxidation of Fe(II) to Fe(III) by Hp was performed with the Fet3p ferroxidase assay described by de Silva *et al.* [42]. Ferroxidase reactions were performed in a 96-well (300 μL) plate such that each reaction mixture contained purified Hp (0.2 μM) in buffer (100 mM sodium acetate trihydrate, 100 μM sodium citrate, pH 5.0) at room temperature. The reaction was initiated by the addition of ferrous ammonium sulfate solution at the indicated concentrations and quenched with the addition of 50 μL of 15 mM ferrozine at 1 min intervals. The concentration of residual Fe(II) was determined from the absorbance of the ferrozine-Fe(II) complex (ε_{562} = 27,900 M^{-1} cm^{-1}).

Ferroxidase activity of Hp was also demonstrated by monitoring the incorporation of Fe(III) into human apo Tf (Sigma-Aldrich). Reactions were carried out in 200 μL of solution containing 6.25 μM apo Tf, 200 μM ferrous ammonium sulfate, and 100 μM sodium ascorbate in 100 mM sodium acetate trihydrate, pH 5.0. Reactions were initiated with the addition of 0.4 μM Hp (except for two controls to which no Hp was added) and proceeded for 1-365 min at 37 °C. The reactions were stopped by transfer to -20 °C. Samples were analyzed by 6% urea PAGE to separate the apo-, mono-, and diferric Tf species [76].

2.15 Statistical Analyses

Samples were prepared in duplicate for the AAA and both values for the amino acid content were presented (Table 3.1). The mean amino acid content of selected amino acid residues from the two samples was used for the determination of the protein content. During the ICP-MS analysis (Section 3.7), a minimum of four replicates was performed for the blank sample and both protein samples. The standard deviation was calculated for both protein samples and converted to the average number of copper or zinc atoms per protein molecule; this converted standard deviation was presented as the error for the measurements. The ferroxidase assays were performed in quintuplicate at each of the indicated substrate concentrations. The standard deviation was calculated from the initial rates at each substrate concentration and presented as the error bars in Figures 3.13A and B. Due to the very small standard deviation values obtained for the non-enzyme catalyzed oxidation of Fe(II) (Figure 3.13A), they were considered negligible and were not used in the determination of error for the enzyme catalyzed oxidation of Fe(II) (Figure 3.13B).

Chapter 3. Results

The majority of the results from this chapter were recently published [77]. I completed all the experiments and received advice from Dr. Grant Mauk for the spectroscopy and ferroxidase studies.

3.1 Expression of Hephaestin in Small Intestine and Brain Tissues

Tissue specific expression of the human *hp* gene was studied experimentally by performing reverse transcriptase-polymerase chain reaction (RT-PCR) on RNA harvested from various tissues or cell lines. Human *hp* RNA was detected in both the brain and the small intestine (Figure 3.1, lanes 1 and 2), but not in an endothelial cell line (Figure 3.1, lane 3).

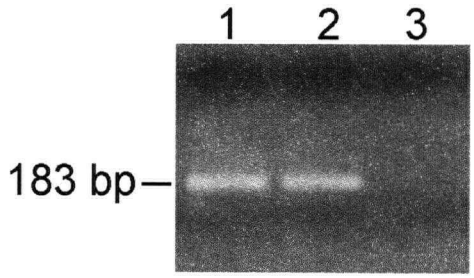

Figure 3.1 RT-PCR to detect expression of *hp*. Human brain (lane 1), small intestine (lane 2), and endothelial cells (lane 3) were used as tissue sources to determine the localization of *hp* expression.

Following this verification, pd$(N)_6$ random hexamers and $(dT)_{12-18}$ oligonucleotides were used to reverse transcribe the duodenal RNA. The large size of the Hp transcript (4,854 bp) necessitated its amplification via PCR in five overlapping segments with each segment containing a unique restriction site for subsequent ligation reactions. After amplification and ligation of the five segments, the entire Hp coding region was cloned into the pBSSK$^-$ plasmid.

3.2 Transient Expression of Recombinant Hephaestin

To express soluble Hp, the putative C-terminal transmembrane region was removed, resulting in a truncated Hp ending at Ser1070. This decision was based on a sequence alignment of the human Hp and human Cp proteins (Appendix A). The resultant Hp polypeptide was one residue shorter than human Cp and residues predicted to be involved in copper binding, disulfide bond formation, and electron transfer were not affected by the truncation. To allow for detection of recombinant Hp, a c-Myc recognition epitope preceded by a FXa cleavage site was added in place of the putative transmembrane spanning region. This Hp-Myc construct was transfected into HEK 293 cells and the resulting transient expression was characterized. A Western blot of both the cellular lysate (Figure 3.2, lane 1) and the conditioned medium (Figure 3.2, lane 2) demonstrated that recombinant Hp was expressed intracellularly. A negative control was performed in which the cells were transfected with only the pcDNA3 vector; a signal was not detected with the anti-Myc antibody in the cellular lysate or the conditioned medium (not shown).

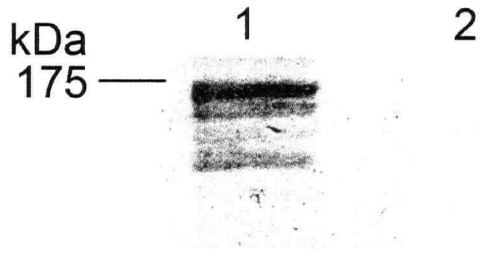

Figure 3.2 Transient expression of the Hp-Myc construct in HEK 293 cells. Recombinant Hp was detected in the cellular lysate sample (lane 1) but not in the conditioned medium (lane 2).

3.3 Expression and Purification of a Soluble Form of Recombinant Hephaestin

As demonstrated by the intracellular localization of the recombinant Hp in the HEK 293 cells, the natural Hp signal peptide may not direct secretion of the protein into the tissue culture medium. Thus, to facilitate secretion, the Hp signal peptide was replaced with the signal peptide and first four residues of human Tf. In addition, to enhance protein detection via Western blotting and facilitate subsequent immunoaffinity purification, the c-Myc epitope was replaced with another immunogenic epitope comprising nine residues from the C-terminus of bovine rhodopsin called epitope 1D4. This new Hp-1D4 construct was transfected into BHK cells. After selection with methotrexate, cells that had stably incorporated the Hp-1D4 construct formed colonies. Ten colonies were selected and expanded into tissue culture flasks. When the cultures were confluent, recombinant Hp was immunoprecipitated from the conditioned medium with anti-1D4 Sepharose 2B resin. The results of the immunoprecipitation (IP) demonstrated that recombinant Hp was secreted into the tissue culture medium by the BHK cells upon incorporation of the human Tf signal

peptide (Figure 3.3). Clones two and five expressed Hp at the highest levels (Figure 3.3, lanes 2 and 5).

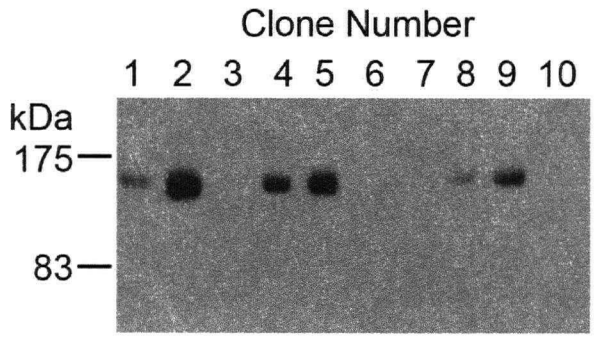

Figure 3.3 Anti-1D4 IP and Western blot of conditioned medium from BHK cultures transfected with the Hp-1D4 construct. As demonstrated by the band intensity, clones two and five secreted recombinant Hp at the highest levels.

Clone five was chosen for expansion into roller bottle cultures as the cells could be maintained in culture for longer periods than those of clone two. The cells were first grown in DMEM-F12 containing NCS and methotrexate. After six days, the roller bottle cultures were confluent and the growth medium was changed to DMEM-F12 containing 2% Ultroser G and 10 μM copper sulfate. Recombinant Hp present in the conditioned medium of the roller bottle cultures was detected by an anti-1D4 Western blot and the amount of secreted recombinant Hp increased with time (Figure 3.4).

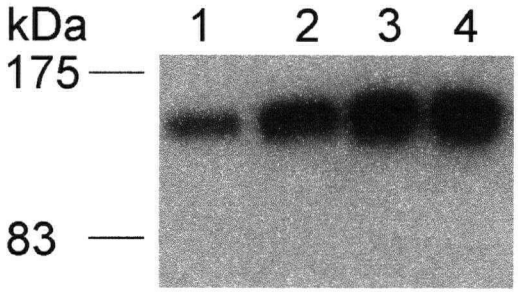

Figure 3.4 Conditioned medium from BHK cells expressing Hp. The medium was collected at days 4 (lane 1), 6 (lane 2), 9 (lane 3), and 12 (lane 4) post passage into roller bottles. Following 10% SDS-PAGE and transfer to a PVDF membrane, the blot was incubated with anti-1D4 primary antibody and anti-mouse secondary antibody and developed with ECL.

During expression, three roller bottles were maintained; each roller bottle contained cells bathed in 200 mL of tissue culture medium. Once the growth media additives were changed from NCS and methotrexate to Ultroser G and copper, the resultant 600 mL of conditioned medium was harvested every three days and recombinant Hp was purified by a one step immunoaffinity purification procedure within 24 hrs of collection. The immunoaffinity purification required one day to complete; the binding and washing steps were performed at 4 °C to preserve both the antigen and antibody while elution of Hp with the 1D4 peptide was performed at room temperature. This method of purification was effective at both purifying and concentrating recombinant Hp (Figure 3.5, compare lanes 1 and 9). Very little recombinant Hp was detected in the unbound fractions (Figure 3.5, lanes 2-8) while pure recombinant Hp was eluted from the immunoaffinity column with the 1D4 peptide (Figure 3.5, lane 9). Regeneration of the immunoaffinity column was completed by three wash steps with alternating low and high pH buffers containing 500 mM NaCl followed by re-equilibration with the starting buffer.

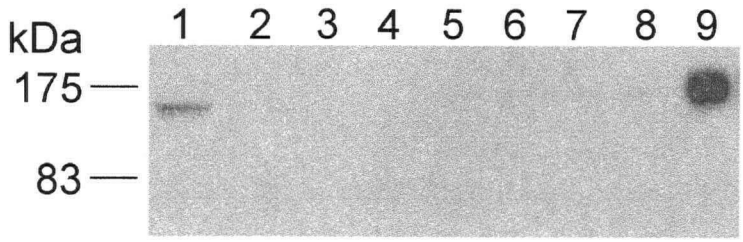

Figure 3.5 1D4 immunoaffinity purification of recombinant Hp. Following 10% SDS-PAGE and transfer to a PVDF membrane, the blot was incubated with anti-1D4 primary antibody and anti-mouse secondary antibody and developed with ECL. Recombinant Hp present in the conditioned medium prior to purification is in lane 1. During purification, the unbound flow through was collected in ~100 mL fractions (lanes 2-8). Purified recombinant Hp eluted with the 1D4 peptide is shown in lane 9; this sample was diluted 10-fold for Western blot analysis.

Following elution of recombinant Hp from the 1D4 immunoaffinity column, the eluants were pooled and the purity was assessed by SDS-PAGE. Preparations of immunoaffinity purified Hp were typically >95% pure (Figure 3.6) and the yield of recombinant Hp from 600 mL of medium was ~1 mg.

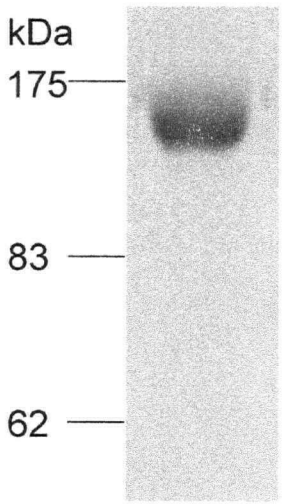

Figure 3.6 SDS-PAGE of purified recombinant Hp. A typical 1D4 immunoaffinity preparation of recombinant Hp yielded protein that was >95% pure. Recombinant Hp (20 μL) that had been eluted from the immunoaffinity column with the 1D4 peptide was visualized by SDS-PAGE and staining with Coomassie blue.

3.4 Amino Terminal Sequence Analysis and Amino Acid Analysis of Recombinant Hephaestin

Based on the cDNA sequence of the Hp-1D4 construct, we predicted the polypeptide sequence of secreted, soluble recombinant Hp would begin at residue Ala24 and include an extra four residues at the N-terminus (VPDK) that are part of mature human Tf protein. As determined by Edman degradation, the N-terminal sequence of recombinant Hp was NH_2-VPDKATRVY- (Ala24 is underlined). This sequence is consistent with the predicted N-terminal sequence of recombinant Hp.

Obtaining an accurate molar absorption coefficient by AAA of recombinant Hp was necessary for subsequent protein concentration determinations by A_{280} measurements. To ensure purity prior to AAA, immunoaffinity purified recombinant Hp was chromatographed

on a Superose 12 column (Figure 3.7). As determined by A_{280} measurements, fractions containing protein were analyzed by SDS-PAGE (Figure 3.7, inset). As verified by Western blot analysis (data not shown), Hp was present in all peaks eluted from the gel filtration column (Figure 3.7, peaks A, B, and C). The most highly concentrated fractions from peak C (Figure 3.7) were pooled and exchanged into 100 mM NH_4OAc buffer, pH 5.0. A UV-visible spectrum of the Hp sample was obtained and the A_{280} was 0.692. Two samples of recombinant Hp were prepared and lyophilized for duplicate AAA analyses. The molar absorption coefficient for recombinant Hp was calculated to be 215,000 M^{-1} cm^{-1} and was based on data from the following amino acid residues: Glx (Glu+Gln), Gly, Ala, and Phe (Table 3.1).

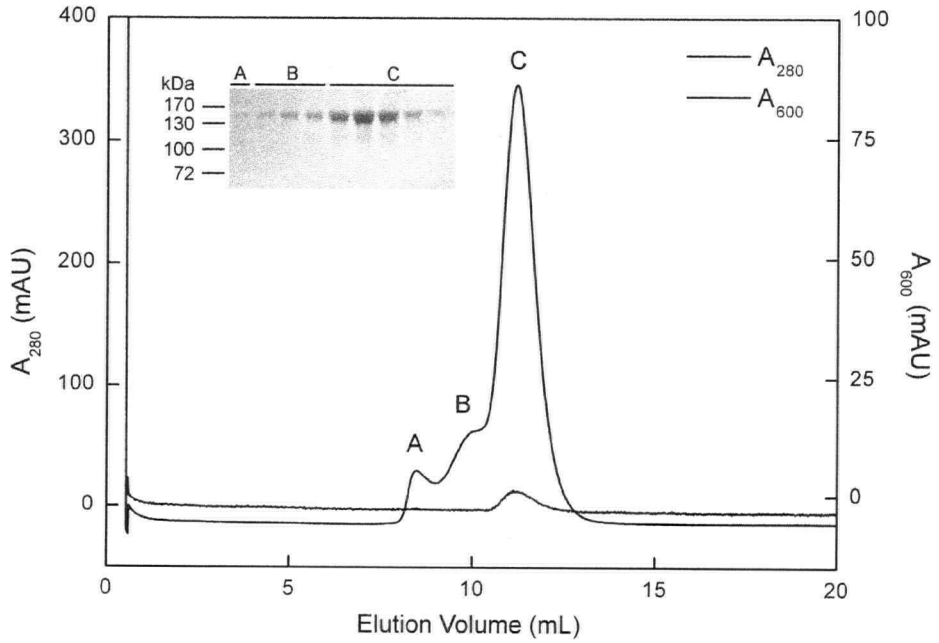

Figure 3.7 Gel filtration of recombinant Hp. To ensure sample homogeneity prior to AAA, immunoaffinity purified Hp was chromatographed on a Superose 12 gel filtration column. Three peaks were observed on the chromatograph (labeled A, B, C). The fractions containing protein were visualized by SDS-PAGE and staining with Coomassie blue (inset).

Table 3.1 AAA data for Hp.

Amino Acid	Amino Acid Content of Each Sample (nmoles)[1]	Amino Acid Composition Predicted from Sequence[2] (number of residues)	Amino Acid Composition Determined Experimentally (number of residues)	Difference Between Predicted and Experimentally Determined Amino Acid Composition (number of residues)
Asx	7.13, 7.13	114	105	9
Glx*[3]	6.99, 7.17	104	104	0
Ser	3.95, 4.05	64	59	5
His	2.47, 2.48	43	36	7
Gly*	6.16, 6.12	90	90	0
Thr	3.56, 3.61	59	53	6
Cys	0.84, 0.74	15	12	3
Ala*	4.90, 5.26	74	74	0
Arg	3.26, 4.05	48	53	-5
Tyr	3.02, 2.87	47	43	4
Val	4.51, 4.49	71	66	5
Met	1.62, 1.39	30	22	8
Phe*	3.64, 3.30	51	51	0
Ile	5.27, 4.17	49	69	-20
Leu	5.69, 5.73	79	84	-5
Lys	1.61, 2.21	42	28	14
Pro	3.73, 3.94	61	56	5

[1]: mean amino acid content of the two samples was used for the determination of the protein content

[2]: Hp sequence was according to NCBI accession number NP_620074 taking into account the sequence modifications described in Section 2.6

[3]: data used to calculate the molar absorption coefficient was from amino acids denoted with *

3.5 Mass Analysis of Recombinant Hephaestin

Potential glycosylation of Hp was investigated by using specific endoglycosidases. Treatment of Hp (2 μg) with the endoglycosidase Endo-H and subsequent SDS-PAGE did

not result in a mobility shift, indicating an absence of high mannose oligosaccharides (Figure 3.8, compare lanes 1 and 2). PNGase F treatment of the same amount of Hp demonstrated a significant reduction in apparent molecular mass from 143,000 Da to 121,000 Da (Figure 3.8, compare lanes 1 and 3), indicating cleavage of hybrid or complex N-linked oligosaccharides.

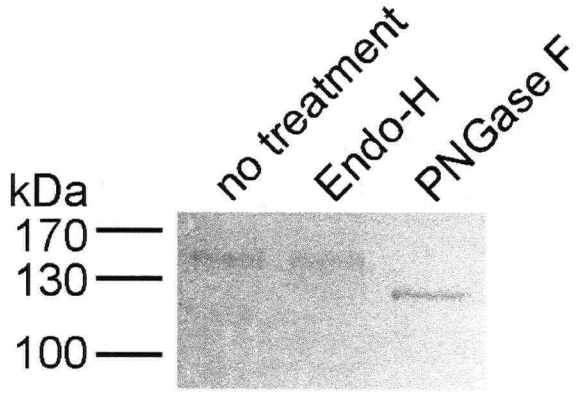

Figure 3.8 Deglycosylation analysis of recombinant Hp. Hp (lane 1) was treated with the glycosidases Endo-H (lane 2) and PNGase F (lane 3) and the samples were visualized by SDS-PAGE and staining with Coomassie blue.

Such heterogeneity of glycosylation is consistent with the complex and uninterpretable electrospray ionization MS analysis of recombinant Hp (data not shown). Therefore, MALDI TOF MS analysis was used to determine the mass of recombinant Hp as 129,600 Da (Figure 3.9).

Attempts were made to treat recombinant Hp with PNGase F and subsequently assess the mass of the deglycosylated protein. Deglycosylation is more effective on a denatured protein, thus heat and SDS were used to denature the protein prior to treatment with the enzyme. MALDI TOF analysis is sensitive to detergents like SDS so the

denatured/deglycosylated sample was precipitated with trichloroacetic acid/acetone and resuspended in dH_20 in an attempt to remove the detergent. However, the protein sample would not co-crystallize with the matrix used for MALDI TOF MS analysis and it was suspected that detergent was still present (data not shown). To circumvent the problem of using a detergent, Hp was deglycosylated in its native form without the addition of SDS. This method required longer incubation times as well as an excess of the PNGase F enzyme. Under these conditions, a band shift was also observed on SDS-PAGE similar to that seen in Figure 3.8 (data not shown). However, analysis of the deglycosylated Hp by MALDI TOF MS was uninterpretable as a signal at the estimated mass (m/z) of Hp was not detected (data not shown).

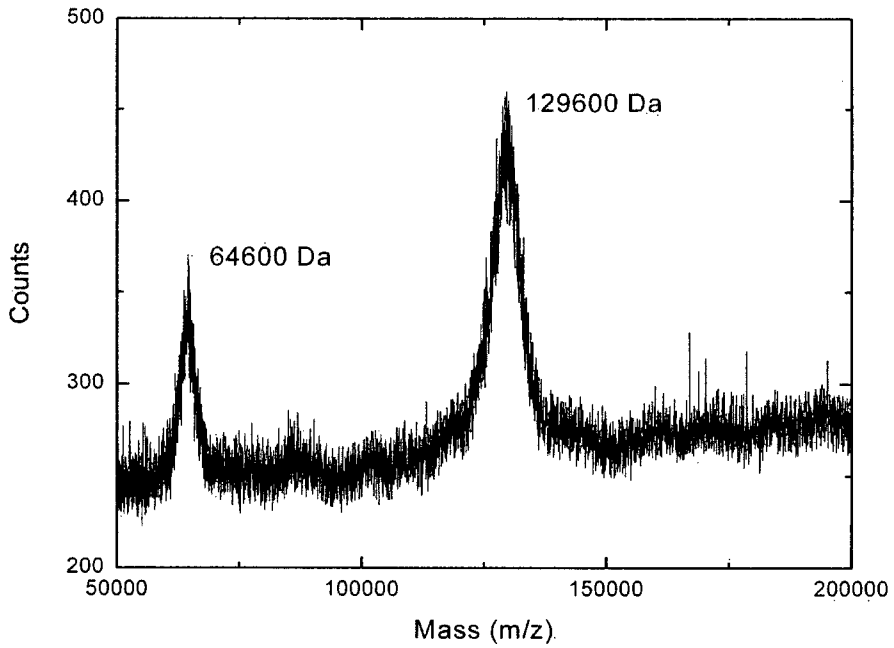

Figure 3.9 MALDI TOF MS analysis of recombinant Hp. The Voyager DE-STR was calibrated externally with IgG. The peak at 64,600 Da is the doubly charged species while the 129,600 Da peak is the singly charged recombinant Hp.

3.6 UV-Visible Spectroscopy of Recombinant Hephaestin

The electronic spectrum of recombinant Hp exhibits an absorbance maximum at 607 nm (2,010 M^{-1} cm^{-1}, Fig. 3.10); this absorption is responsible for the predicted blue color of Hp (Fig. 3.10, inset).

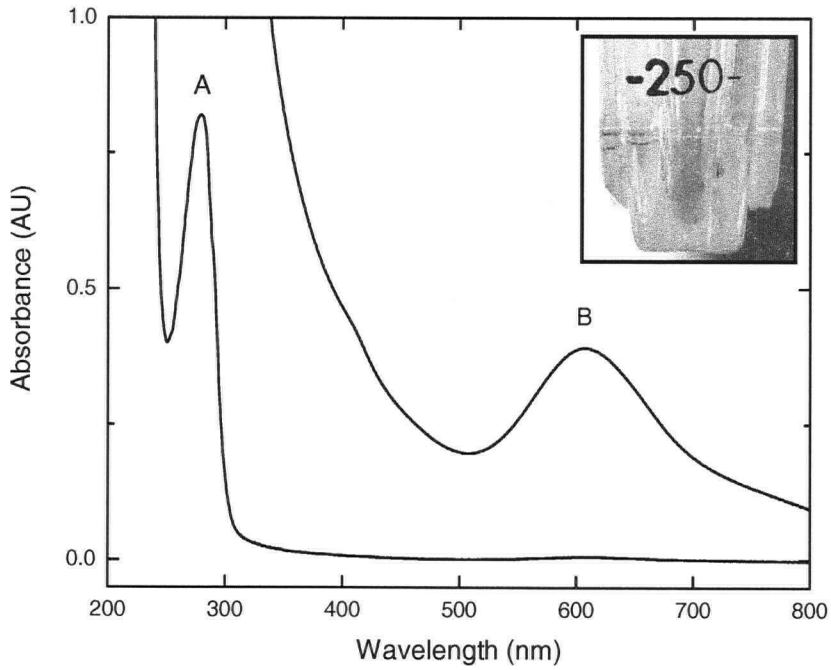

Figure 3.10 UV-visible spectrum of recombinant Hp. Trace A represents Hp at a concentration of 4 μM while the Trace B is of Hp at a concentration of 194 μM. Inset shows a micro-concentrator containing purified human Hp (~230 μM).

Due to the number of *d*-orbital electrons in the reduced *versus* oxidized copper atoms ($3d^{10}$ and $3d^{9}$, respectively), only Cu(II) atoms incorporated into T1 sites will display the visible absorbance at ~600 nm. Because of the low molar absorptivity of purified Hp compared to human Cp [64, 78], it was hypothesized that some of the T1 copper atoms may

be reduced. To ensure the T1 copper atoms were oxidized in the purified Hp, a sample was treated with hydrogen peroxide and UV-visible spectra were obtained. The addition of hydrogen peroxide did not alter the absorbance in the visible region of the spectrum (data not shown); thus, the purified recombinant Hp appeared to be in an oxidized state, at least as far as could be determined from the UV-visible spectroscopy of the T1 copper atoms. This oxidized state was reversible when sodium ascorbate was added as a reducing agent. Upon addition of a large excess of sodium ascorbate to purified Hp, the T1 copper atoms were reduced as indicated by the loss of the absorbance at 607 nm (Figure 3.11A). Immediately following removal of the sodium ascorbate by buffer exchange, the T1 copper atoms were beginning to oxidize from the presence of ambient oxygen. Hydrogen peroxide was added and the blue copper atoms were re-oxidized. The absorbance at 607 nm did not reach the original absorbance as small amount of protein were lost in each round of buffer exchange (Figure 3.11B). This reduction-oxidation cycle could be repeated (data not shown).

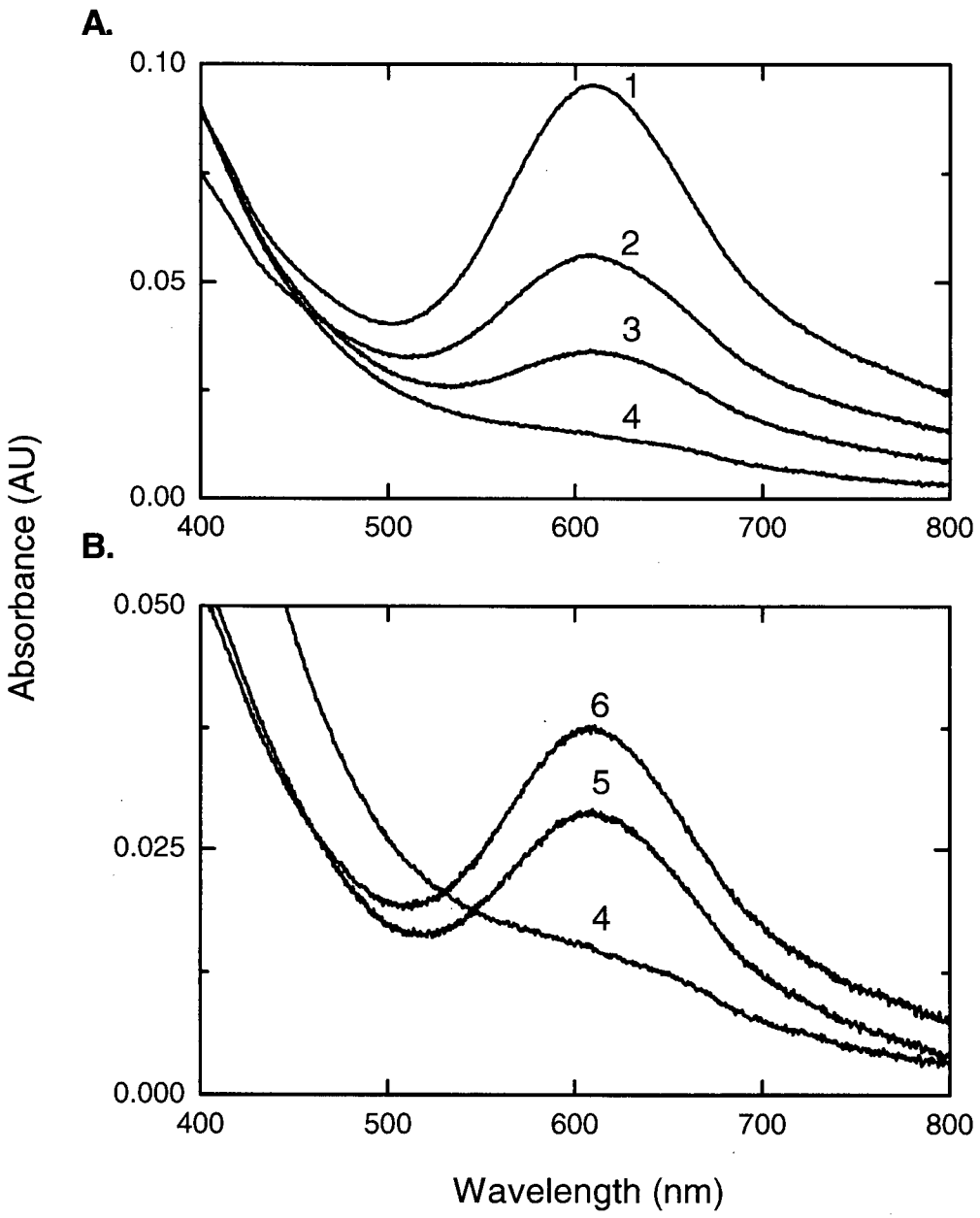

Figure 3.11 Reduction and oxidation of the T1 copper atoms in recombinant Hp. A. Reduction of recombinant Hp with sodium ascorbate. Trace 1 is purified, recombinant Hp. Trace 2 was obtained after the addition of 30 equivalents of sodium ascorbate. Traces 3 and 4 were obtained after the addition of 1,000 equivalents of sodium ascorbate after 10 and 30 min incubations, respectively. **B.** Oxidation of recombinant Hp with hydrogen peroxide. Trace 4 was described above. Trace 5 was obtained immediately following removal of the sodium ascorbate by buffer exchange. Trace 6 was obtained following the addition of 30 equivalents of hydrogen peroxide accompanied by a 10 min incubation.

3.7 Copper Content of Recombinant Hephaestin

ICP MS was used to determine the copper content of purified Hp with copper-loaded human Tf as a control. The instrument was calibrated with a multi-element standard (Figure 3.12). Samples were spiked with a commercially available selenium standard and values were normalized to this standard (results are the average of at least 3 analyses). Copper-loaded Tf contained an average of 1.98 ± 0.04 copper atoms per protein molecule; this result agrees well with the expected value of 2 Cu atoms/Tf molecule [79]. Hp was found to have an average of 3.13 ± 0.03 copper atoms per protein molecule; based on the number of putative copper binding sites in the Hp sequence, the expected value is 6 copper atoms/Hp molecule [58]. A small amount of zinc (0.60 ± 0.04 Zn atoms per protein molecule) was also detected in the sample of recombinant Hp.

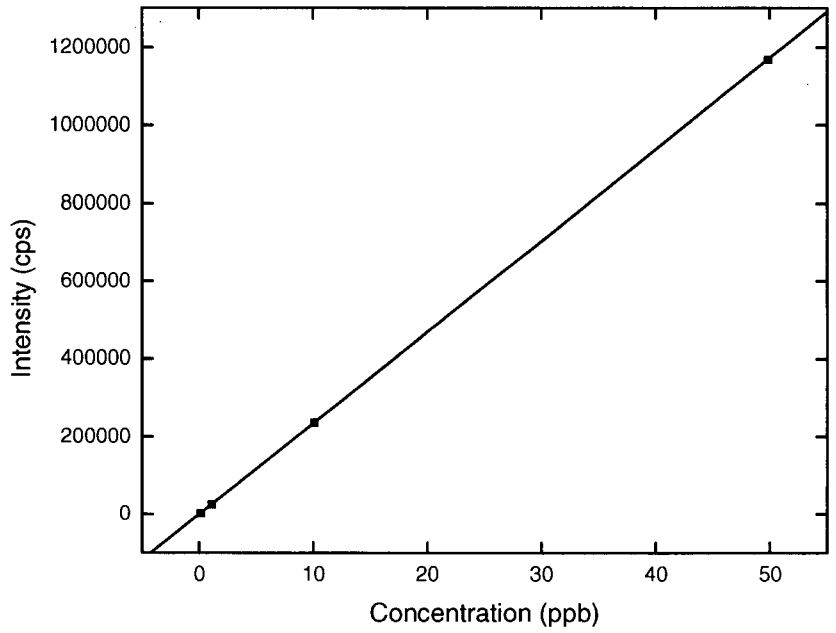

Figure 3.12 Representative ICP MS calibration curve for ^{63}Cu. Linear regression (solid line) demonstrated that the data points followed a linear trend over a large dynamic range (0.1 ppb to 50 ppb).

Previous studies have shown that the reconstitution of the MCOs Cp and Fet3p requires copper in the reduced form [42, 80], thus Cu(II)SO_4-ascorbate was used in an effort to reconstitute Hp with more copper atoms. A 1,000-fold excess of the reducing agent, sodium ascorbate was first added to the Hp sample. An immediate and significant reduction in the absorbance at 607 nm was observed similar to that in Figure 3.11A. The addition of Cu(II)SO_4 (up to a maximum of a 10-fold molar excess), even after a 30 min incubation, did not change the absorbance at 607 nm (data not shown). This attempt to increase the copper occupancy of recombinant Hp was considered unsuccessful.

3.8 Ferroxidase Activity of Recombinant Hephaestin

Using Fe(II) as a substrate, the kinetic parameters of the ferroxidase activity of purified Hp were determined. Ferroxidase activity assay mixtures contained 0.2 μM Hp in 100 mM sodium acetate trihydrate/100 μM sodium citrate buffer (pH 5.0, the optimal pH for Hp ferroxidase activity (data not shown), at room temperature). The reaction was initiated by the addition of varying concentrations of freshly prepared ferrous ammonium sulfate solution and was quenched by addition of ferrozine solution (15 mM) at 1 min intervals. Substrate depletion was determined from the residual absorbance of the ferrozine-Fe(II) complex. Heat inactivated recombinant Hp was used as a negative control; as expected, this protein exhibited no ferroxidase activity (data not shown). All ferroxidase reactions were corrected for background auto-oxidation rates of Fe(II) (Figure 3.13A); thus, the kinetic parameters reported here represent the Hp catalyzed conversion of Fe(II) to Fe(III) (Figure 3.13B). An Eadie-Hofstee plot was used to determine the K_m (2.1 μM) and V_{max} (0.5 μM min^{-1}) for this reaction (Figure 3.13C). These parameters were then used to simulate the observed kinetic results (Figure 3.13B, solid line). This model indicates that the data conform to Michaelis-Menten kinetics. Substrate inhibition was observed at the highest concentration of Fe(II) (Figure 3.13B); therefore, this value was not used in the generation of the Eadie-Hofstee plot.

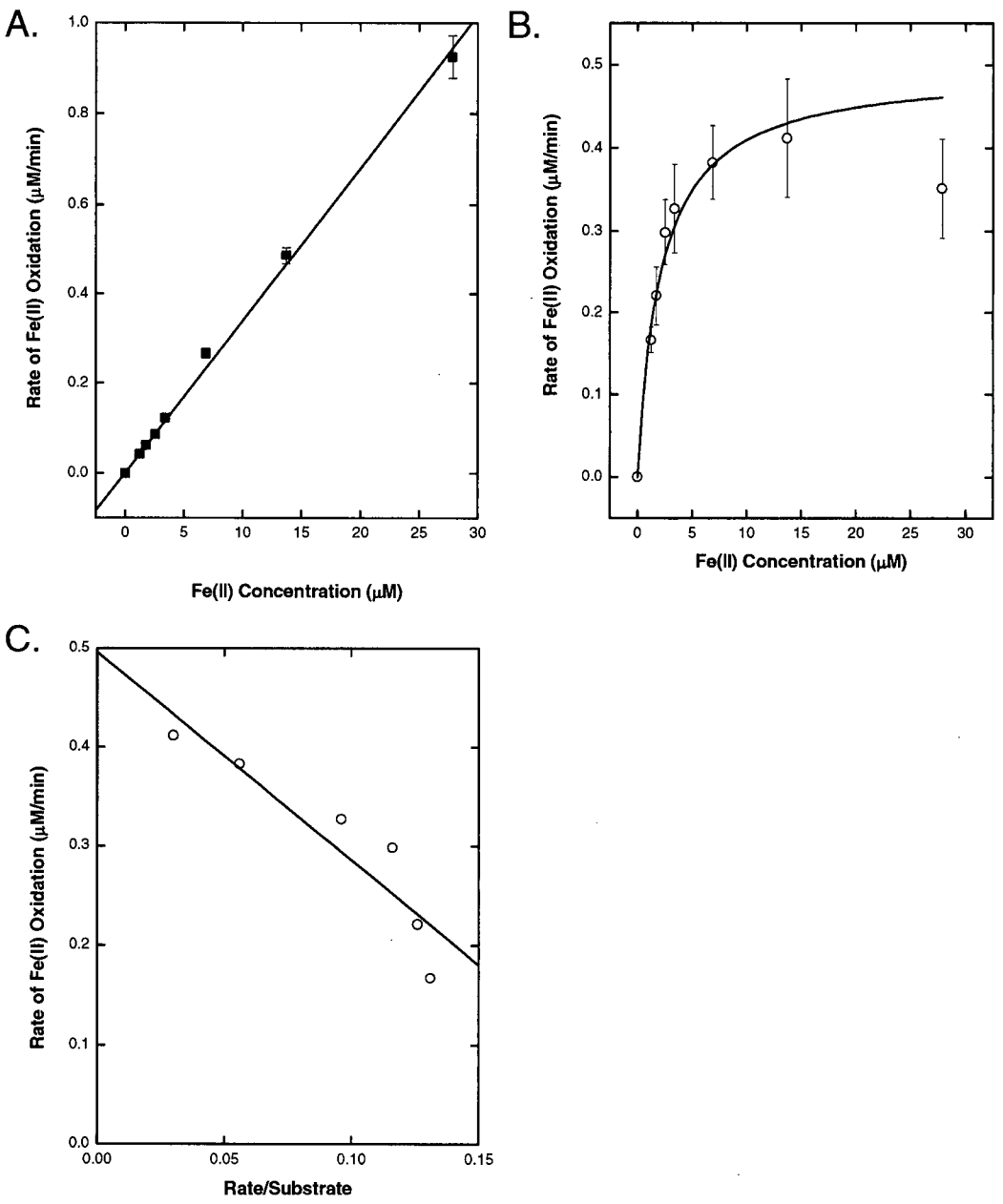

Figure 3.13 Ferroxidase activity of recombinant Hp. A discontinuous ferroxidase assay was performed to obtain the catalytic constants K_m and V_{max} for Hp. **A.** Non-enzyme catalyzed oxidation of Fe(II). **B.** Velocity *versus* substrate curve for Hp catalyzed oxidation of Fe(II) was determined as described in Materials and Methods. Error bars represent 1 S.D. **C.** Eadie-Hofstee plot used to determine K_m and V_{max} for the data shown in **B**. The data point at the highest substrate concentration in **B** was not used in the Eadie-Hofstee plot.

3.9 Interactions Between Recombinant Hephaestin and Human Transferrin

Roy and Enns [81] suggested that the intestinal ferroxidase activity of Hp may be necessary to facilitate the loading of apo Tf with ferric iron for subsequent transport in blood to tissues. To assess this hypothesis, reaction mixtures containing apo Tf and ferrous iron were incubated at 37 °C for varying times in the presence or absence of Hp, and the reactions were then terminated by freezing at -20 °C. Samples were analyzed by urea PAGE, a technique that separates Tf species based on ferric iron content [76]. After more than 6 hrs at 37 °C in the absence of Hp, very little apo Tf was converted to mono- or diferric Tf (Figure 3.14, lanes 1 and 2). As apo Tf does not bind Fe(II), this result suggests that auto-oxidation of Fe(II) to Fe(III) during this reaction period was minimal. However, under the same experimental conditions but in the presence of Hp, more than half of the apo Tf was converted to mono- and diferric Tf after 1 hr, and conversion to diferric Tf was complete after 365 min (Figure 3.14, lanes 3-10). These results establish that Hp catalyzes the oxidation of Fe(II) to Fe(III) and promotes the conversion of apo Tf to diferric Tf.

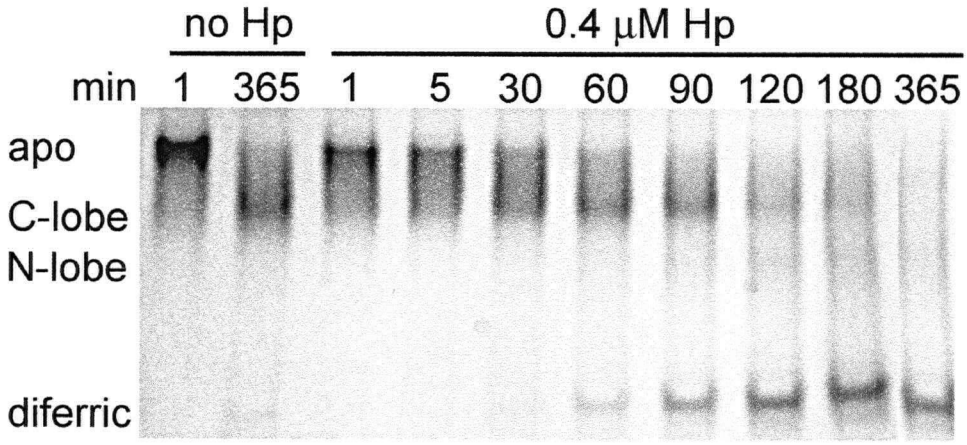

Figure 3.14 Oxidation of Fe(II) by Hp and incorporation of Fe(III) by human apotransferrin. Samples were incubated for the times indicated and analyzed by 6% urea PAGE to separate the apo-, mono-, and diferric transferrin species. Lanes 1 and 2 were controls to which no Hp was added. Lanes 3-10 were experimental samples that contained 0.4 μM recombinant Hp.

Chapter 4. Discussion

4.1 Expression and Purification of Recombinant Human Hephaestin

Prior to cloning the human *hp* gene for recombinant expression, the tissue specific expression of *hp* was studied by RT-PCR. Human *hp* was found to be expressed in the brain and small intestine, but not by an endothelial cell line (Figure 3.1). This expression pattern is consistent with that described by others [57, 58]. High levels of *hp* expression in the duodenum support its role as the intestinal ferroxidase and are consistent with the observation that mice harboring the *sla* mutation (resulting in non-functional Hp) develop a hypochromic, microcytic anemia. However, the expression of *hp* in other tissues, like the brain, is harder to explain. It is also unclear why both *cp* and *hp* are expressed in the brain [58, 82]. The requirement for two homologous ferroxidases in the brain seems redundant. In addition, Cp found in the astrocytes of the brain is also anchored to the membrane [82]. In contrast to Hp, Cp does not have a transmembrane spanning domain but is anchored by a glycosylphosphatidylinositol addition [82]. Hp and Cp have also been shown to be present in the retinal pigment epithelium [62]. In humans with aceruloplasminemia, severe iron overloading in the CNS is detected but in mouse, both Cp and Hp have to be absent to see the same levels of CNS iron overloading. The work by Hahn *et al.* [62] is the first and only study to demonstrate that perhaps Cp and Hp work in concert to facilitate iron export from the retinal pigment epithelium in the CNS.

Following verification that Hp mRNA could be detected by RT-PCR of human duodenal tissue, Hp cDNA was reverse transcribed and cloned into the expression vector pcDNA3. The Hp coding region was truncated at Ser1070, such that the putative

transmembrane spanning region was removed (Appendix A) and replaced with a FXa cleavage site and the c-Myc 9E10 epitope, the latter to allow for detection and purification.

The Hp-Myc construct was transfected into HEK 293 cells for transient expression. Transient expression was initially chosen as a rapid method to verify Hp production and detection. We predicted that removal of the transmembrane region would facilitate extracellular secretion by the HEK 293 cells, as this approach has proven successful for recombinant expression of Fet3p [66]. However, simply removing the putative transmembrane region was not sufficient for extracellular secretion (Figure 3.2) as recombinant Hp was detected exclusively in the cellular lysate. This observation is consistent with that of Li and colleagues [63] who found that mouse Hp lacking the transmembrane domain was expressed and glycosylated, but not secreted by *S. cerevisiae*. It is unknown why multiple bands were recognized by the anti-Myc antibody (Figure 3.2, lane 1); however, the bands may represent differences in glycosylation, proteolytic breakdown of recombinant Hp, or endogenous HEK 293 proteins that are recognized by the anti-Myc antibody. To facilitate extracellular secretion of recombinant Hp, another approach was undertaken.

In our laboratory, numerous studies have shown that the signal peptide and first four amino acids of human transferrin, a soluble plasma glycoprotein, facilitate high levels of secretion of recombinant proteins from BHK cells [76, 83, 84]. Thus, the Hp signal peptide was replaced with the signal peptide and first four amino acids of human transferrin. Also, the C-terminal c-Myc recognition epitope was replaced with the 1D4 epitope to simplify both detection during Western blotting and subsequent purification of recombinant Hp. Upon transfection of this new Hp construct into BHK cells, a soluble, secreted form of Hp

was expressed and could be detected in an anti-1D4 immunoprecipitation of the tissue culture medium (Figure 3.3). Why the presence of the human Tf signal sequence facilitated the secretion of recombinant Hp when the native Hp signal peptide did not is unknown as the signal peptide is removed in the endoplasmic reticulum by signal peptidase during protein synthesis and is not thought to be involved in protein secretion or membrane insertion.

BHK cell cultures can be grown in a large capacity in roller bottle culture systems (1700 cm^2 surface area). As BHK cells are adherent, the conditioned medium can be collected from the roller bottles at suitable intervals and replaced with fresh growth medium; this can continue until the cells eventually begin to detach from the roller bottle surface and die. Typically, the BHK cells expressing Hp were maintained for at least 2-3 weeks before cell detachment and death became significant. Hp levels were detected by Western blot from samples collected during each tissue culture medium change (every three days). The levels of Hp secreted by the BHK cells into the cell culture medium increased with time (Figure 3.4). The switch from newborn calf serum to the serum replacement, Ultroser G, was performed to decrease the levels of other proteins, especially albumin, and to facilitate purification; it has also been observed that Ultroser G increases the production of recombinant protein expression possibly by stressing the cells (personal communication, Anne Mason and Ross MacGillivray). However, the cellular mechanisms involved in this increased expression level are currently not understood.

Purification of Hp by anti-1D4 immunoaffinity chromatography afforded the convenient purification of the protein in a single day. Very little Hp was detected in the unbound fractions (Figure 3.5, lanes 2-8). Compared to its concentration in the tissue culture medium (Figure 3.5, lane 1), the purified Hp was concentrated by a significant amount upon

elution from the column with the 1D4 peptide (Figure 3.5, lane 9). Recombinant Hp exhibited no evidence of proteolytic degradation during purification as determined by the single band present on an SDS-PAGE/Coomassie blue gel (Figure 3.6). The purified, concentrated protein retained ferroxidase activity after storage at -70 °C for at least 1 month. Notably, the arginyl and lysyl residues (Appendix A) known to render human Cp [64] susceptible to proteolysis [85, 86] during purification [87] are not conserved in the sequence of Hp. Thus, Hp may prove to be a more robust multicopper oxidase for structural and kinetic studies.

Although the immunoaffinity purification scheme used to purify recombinant Hp was effective, it was very time consuming as the protein had to be purified from the tissue culture medium within 24 hrs to prevent bacterial growth in the tissue culture growth medium. Sodium azide, a commonly used inhibitor of bacterial growth, is an inhibitor of the enzymatic activity Cp and is likely to inhibit Hp; thus it was not used in these studies. As medium was collected every three days, purification of recombinant Hp was performed every three days for the entire time period the BHK cells were alive and producing protein. Also, it was relatively expensive to prepare and elute from the immunoaffinity column. A very small column was used in these studies (bed volume: 10 mL) such that the binding capacity of the recombinant Hp was limited. However, the elution of recombinant Hp from the column with the 1D4 peptide represents a very gentle elution method especially when compared to elution procedures utilizing chaotropic agents or extremes of pH. In the future, it would be beneficial to attempt purification with a different affinity tag (such as a six histidine tag) that was not based on an antibody-antigen system. I have made Hp constructs with an N-terminal six histidine tag in place of the 1D4 tag and generated stable BHK

transfectants, but Western blots have not yet been performed to assess expression of recombinant Hp. It will be of importance to determine if the six histidine tag (commonly purified with the use of a nickel column) affects copper binding by Hp.

4.2 Molar Absorption Coefficient (ε_{280}) and Gel Filtration Chromatography

Quantitative AAA was used to obtain an accurate molar absorption coefficient (ε_{280}) for recombinant Hp. As we were not in possession of antibodies against recombinant Hp and the antibodies used in other studies were to the C-terminal region of Hp [59] that was removed in our study, a sandwich ELISA analysis for protein concentration determination was not an option. The molar absorption coefficient obtained for recombinant Hp was ε_{280} = 215,000 M^{-1} cm^{-1}. This compares well to the theoretical molar absorption coefficient (ε_{280} = 197,000 M^{-1} cm^{-1}) that was calculated based on the method described by Pace [88].

Prior to sample submission for quantitative AAA, immunoaffinity purified Hp was subjected to gel filtration on a Superose 12 column. Three peaks were observed on the resultant chromatogram (Figure 3.7) and all peaks contained Hp (Figure 3.7, inset). The three peaks may represent populations of Hp differing in their copper content. In a previous study by Musci *et al.* [80], holo Cp was separated from apo Cp by anion exchange chromatography with a Mono Q column. It is also possible that populations of Hp, differing in their complements of N-linked glycans, exist and may also account for the observed gel filtration elution profile.

4.3 Mass Analysis

The predicted mass of Hp with the first four amino acids of human Tf and the FXa cleavage site/1D4 epitope is 119,580 Da. The mass of recombinant Hp obtained by MALDI TOF analysis (Figure 3.9, 129,600 Da) is consistent with glycosylation of Hp. The difference in the experimentally determined and predicted molecular masses is ~7.7% and this compares well to the ~8% carbohydrate present on human Cp [89]. The low signal observed in the MALDI TOF MS analysis (Figure 3.9) is commonly observed with glycosylated proteins as the heterogeneity attributed to the presence of the sugars can lead to signal suppression. Similar MALDI TOF MS results have been obtained for both human and bovine Cp [90].

While recombinant Hp exhibited no change in apparent mass following treatment with the endoglycosidase Endo-H and SDS-PAGE, treatment with PNGase F reduced the apparent mass of the protein (Figure 3.8). These observations indicate that recombinant Hp has been modified with hybrid or complex N-linked glycans. Related observations were reported by Nittis and Gitlin who found that endogenous human Hp from a colorectal adenocarcinoma cell line is synthesized as a single polypeptide and modified by PNGase F-sensitive N-linked glycans [91]. Recombinant Hp has eight predicted N-linked glycosylation sites, but only two residues, N164 and N714, are probable candidates for glycosylation (http://www.cbs.dtu.dk/services/NetNGlyc/ and [58]). Recombinant Hp is unlikely to possess O-linked glycans [92], so the discrepancy between the experimental and predicted masses probably results from N-linked glycosylation or some additional form of post-translational modification.

4.4 Electronic Spectroscopy and Copper Content

Purified recombinant Hp exhibited an absorbance maximum at 607 nm with a molar absorptivity of 2,010 M^{-1} cm^{-1} that is responsible for the blue color typical of multicopper oxidases and other proteins having a T1 copper site. As discussed previously, Hp was predicted to have three T1 copper sites, so the low intensity of this maximum may be interpreted as indicating that only 10-15% of the T1 copper sites in the recombinant Hp are occupied. This conclusion is based on two assumptions: (1) the anticipated molar absorptivity of a single T1 copper site is 4,000-5,000 M^{-1} cm^{-1} [78], and (2) all of the T1 copper sites in the Hp samples used to obtain the spectrum shown in Figure 3.10 were oxidized. Incomplete oxidation of the T1 copper sites of human Cp can result in a deceptively low molar absorptivity (7,000 M^{-1} cm^{-1}) that is increased to 9,000 M^{-1} cm^{-1} with the addition of oxidants [64]. This resulting value for the human protein remains anomalously low apparently because one of the three T1 copper sites of human ceruloplasmin has a sufficiently high reduction potential that it is permanently reduced [46]. Consequently, the molar absorptivity of the T1 maximum at 610 nm of human Cp (9,000 M^{-1} cm^{-1}) is about one-third lower than that of chicken ceruloplasmin (12,930 M^{-1} cm^{-1}), a species of ceruloplasmin for which none of the three T1 copper sites has such a high reduction potential [93]. Considering that the structural basis for the high potential T1 site of human Cp is the replacement of a Met ligand with a Leu residue [46] and that no sequence anomaly of this type pertains to human Hp (Appendix A), the presence of a permanently reduced T1 site in this protein seems highly unlikely. Treatment of recombinant Hp with an excess of hydrogen peroxide had no effect on the intensity of the visible transition (λ_{max} = 607 nm), thus the blue T1 copper atoms were considered to be fully oxidized in the sample

of purified Hp. The low molar absorptivity (ε_{607} ~2,010 M^{-1} cm^{-1}) likely reflects the incomplete occupancy of the copper sites of recombinant Hp.

ICP MS analysis of the recombinant Hp indicated the presence of an average of 3.13 copper atoms/protein molecule rather than the six copper atoms anticipated, yet Hp prepared in this manner possesses ferroxidase activity (*vide infra*). As this activity presumably requires the presence of a trinuclear copper site and a minimum of one T1 copper, at least some of the Hp present in samples prepared as described here must possess a minimum of four copper atoms distributed in this manner. It is possible that recombinant Hp has unoccupied copper binding sites or that other *d*-block metals, such as zinc, nickel, or cadmium, have occupied the copper sites [94]. In fact, a small amount of zinc, a non-redox-active metal, was detected by ICP MS analysis in the recombinant Hp sample.

Initial efforts to increase occupancy of the copper binding sites in recombinant Hp by treatment with copper sulfate and sodium ascorbate appeared to be unsuccessful (data not shown). The immediate and significant reduction of the absorbance at 607 nm by addition of sodium ascorbate could not be reversed with the addition of excess of $Cu(II)SO_4$. However, based on studies of the redox cycling ability of the T1 copper atoms, it is probable that removal of the sodium ascorbate by buffer exchange or dialysis is required to achieve an increase in the intensity of the visible transition. The presence of excess sodium ascorbate has been shown to maintain the T1 copper atoms in the Cu(I) state leading to a reduced visible transition (Figure 3.11A); reappearance of the visible transition was not observed until the sodium ascorbate was removed by buffer exchange (Figure 3.11B). Additionally, in view of the apparent structural similarity of Hp and Cp and the complex procedure required for reconstitution of Cp with copper [80, 95], reconstitution of Hp with copper may require a

similarly complex protocol. This has not yet been assessed and is outside the scope of this thesis.

4.5 Ferroxidase Activity

Prior to this study, Hp was shown indirectly to possess oxidase activity towards both inorganic iron and organic amine-containing substrates [60]. In this previous report, however, activity assays were not performed with purified Hp and kinetic parameters were not reported. We have used a discontinuous ferroxidase assay to determine the K_m (2.1 μM) and V_{max} (0.5 μM min^{-1}) of purified recombinant Hp with respect to ferrous ammonium sulfate as a substrate. The K_m for Fe(II) observed in this study is comparable to previous observations for soluble, recombinant *S. cerevisiae* Fet3p (4.8 or 5.4 μM) [66, 96] and human Cp (0.6 μM) [97]. However, the V_{max} and subsequently the k_{cat} are lower; in fact, Hp has the lowest k_{cat} for Fe(II) to Fe(III) turnover of the listed multicopper oxidases (Table 4.1). The low rate of Fe(II) oxidation presumably results from insufficient copper incorporation into the recombinant Hp, consistent with the observation that addition of copper to *S. cerevisiae* Fet3p increased the V_{max} without changing the K_m [42].

Interestingly, the k_{cat} values for both *S. cerevisiae* Fet3p and Hp differ markedly from those of plasma-derived human Cp and *P. pastoris* Fet3p (Table 4.1). To date, there is much variability in the kinetic parameters presented for the multicopper ferroxidases and this may be partly attributed to the variety of sources:

1. Hp (present study) and *S. cerevisiae* Fet3p [66] were obtained from recombinant sources and were expressed without their transmembrane spanning regions,

2. *S. cerevisiae* Fet3p was also purified from yeast cell membranes [42],

3. Human Cp was purified from plasma [97],

4. Full length *P. pastoris* Fet3p was purified from both a membrane preparation and released from the cell membranes by limited proteolysis [65].

As such, it is exceedingly difficult to make a meaningful comparison of the catalytic parameters between the different multicopper ferroxidases and even between the same proteins from different species. It will likely be more informative to assess various recombinant Hp preparations with respect to kinetic parameters of ferroxidase activity, such as (1) those containing the predicted six copper atoms (full occupancy), (2) those with various mutations designed to affect ferroxidase activity, and (3) full length Hp *versus* the soluble, truncated protein.

A range of Fe(II) concentrations (from $0.6K_m$ to $13K_m$) was used to generate a velocity *versus* substrate concentration plot of Hp catalyzed ferrous oxidation (Figure 3.13A). From this analysis, it appears that the enzyme reaction is subject to substrate inhibition as reaction rates started to decline at Fe(II) concentrations greater than 15 μM. To date, substrate inhibition by Fe(II) has not been discussed for any of the other multicopper ferroxidases although substrate inhibition appears to have been observed in an iron uptake study involving Fet3p [98]. Fe(II) must be oxidized prior to uptake by the permease Ftr1p into the yeast cell, so iron uptake is an indirect measure of Fe(II) oxidase activity by Fet3p. At approximately 5 μM Fe(II) concentration, the rate of iron uptake began to decline and subsequently plateau when membrane preparations of wild type *S. cerevisiae* were used as a source of Fet3p. The authors do not discuss why this might have occurred [98]. The reason

for the substrate inhibition observed in this study is presently unknown, although it may be possible that two Fe(II) molecules are binding near the active site(s) of Hp subsequently leading to the formation of an unproductive complex. The substrate inhibition may simply be a facet of the natural cellular environment encountered by native Hp as it is unlikely that the intracellular free iron pool will reach concentrations of 15 μM (a study by O'Halloran's group suggests that less than one free copper atom exists in intracellular environments [99]). It will be of interest to assess the ferroxidase activity and substrate inhibition of recombinant Hp when the integral copper binding sites are fully occupied.

Table 4.1 Catalytic constants for the multicopper ferroxidases Fet3p, Hp, and Cp determined by steady-state kinetic analyses.

Protein	Species	Protein Source	k_{cat} (min^{-1})	Ref.
Fet3p	*S. cerevisiae*	full length, purified from *S. cerevisiae* membranes	2.6	[42, 66]
Fet3p	*S. cerevisiae*	soluble, recombinant	9.5	[66, 96]
Fet3p	*P. pastoris*	full length, purified from *P. pastoris* membranes	335	[65]
Fet3p	*P. pastoris*	soluble, released from *P. pastoris* membranes by limited proteolysis with trypsin	1070	[65]
Hp	*H. sapiens*	soluble, recombinant	2.5	this study
Cp	*H. sapiens*	plasma-derived	550	[97]

4.6 Interactions with Human Transferrin

The ferroxidase activity of Hp was also manifested by the ability of Hp to promote the formation of diferric Tf upon incubation of the protein with apo Tf and Fe(II). Under identical conditions, incubation of apo Tf and Fe(II) without Hp resulted in formation of

little or no diferric Tf (Figure 3.14). Given the localization of Hp to the basolateral membrane of duodenal enterocytes [61], this result is consistent with a role for Hp as the ferroxidase that catalyzes the oxidation of Fe(II) on the serosal side of the enteric epithelium for loading of Fe(III) onto apo Tf. A possible requirement for a physical interaction between Hp and Tf to facilitate iron transfer remains to be evaluated, but it is likely that Fe(III) released from Hp must be bound immediately by Tf or another Fe(III) acceptor to avoid the insolubility of Fe(III) at physiological pH and O_2 concentrations [3]. Mutant Hp that exists in enterocytes of *sla* mice also exhibits ferroxidase activity [60], albeit at a reduced level. However, the location of the mutant protein changes from basolateral and intracellular (observed with the wild type protein) to strictly intracellular [61]. This observation also supports the hypothesis that a physical interaction between Hp and Tf likely exists to facilitate iron transfer between the two proteins - the strictly intracellular localization of the *sla* Hp may preclude interaction with Tf, ultimately preventing delivery of Fe(III) and leading to an anemic phenotype observed in the *sla* mouse.

4.7 Future Directions

The present study describes the expression and characterization of human Hp and provides a baseline for future studies. Of primary importance is the copper status of recombinant Hp. The kinetic parameters for the ferroxidase activity of Hp will be more representative of the physiological processes if the recombinant protein is fully loaded with copper. To establish an efficient and reproducible method for fully loading the recombinant Hp, copper depletion and reincorporation studies could be performed in accordance with a variety of conditions known to promote copper loading in other multicopper ferroxidases

[42, 80, 95]. To assess the uptake and coordination of the integral copper atoms, UV-visible spectroscopy and ICP MS techniques could be used as described previously.

Other important aspects of human Hp are the amino acid residues that contribute to integral copper atom coordination, electron transfer, and substrate binding – these will be discussed in turn (Table 4.2). A unique feature of Hp that sets it apart from both Cp and Fet3p is the presence of a methionyl residue coordinating the T1 mononuclear copper atom of domain 2. This residue in Fet3p and in the homologous domain of Cp is a leucyl residue. Studies of human Cp have indicated that the leucyl residue provides a high reduction potential to the associated T1 copper atom. This observation led to the prediction that the domain 2 mononuclear copper atom is redox inactive and does not participate in the enzymatic activity of the protein [46]. To observe the effect(s) of a Met→Leu substitution on the UV-visible spectroscopic and kinetic properties of recombinant human Hp, the M357L mutant has been generated and is awaiting transfection and expression. It is difficult to predict what the outcome of this mutation will be. The reverse Leu→Met substitutions have been studied in *S. cerevisiae* Fet3p and human Cp and in all cases, the oxidase activities of the mutant proteins were unaffected [51, 64, 98].

As may be inferred from the human Cp crystal structure [100], electrons generated from the oxidation of Fe(II) are believed to travel from the mononuclear T1 copper atoms in domains 2 and 4 to the mononuclear T1 copper atom in domain 6 prior to reaching the trinuclear cluster via the following pathways (the one letter amino acid code is used, numbering according to Appendix A):

Cu2-H343...H-bond...E652-A653-D654-V655-H656-Cu4

Cu2-H295-V294-D293-V292-E291...H-bond...H1045-Cu6

Cu4-H704...H-bond...E990-I991-D992-L993-H994-Cu6

Similar electron transfer pathways can be predicted for human Hp based on the sequence similarity with human Cp. To determine if Hp utilizes these same electron transfer pathways, mutants have been designed and the kinetic parameters of iron oxidation (performed as described previously) and the oxidation of organic amine compounds [51] by the recombinant mutant Hp proteins could be assessed. Although potential electron transfer pathways exist from the domain 2 copper atom to the mononuclear sites in domains 4 and 6, the likelihood of electron transfer occurring from domain 2 has been questioned due to the high reduction potential of this site in human Cp that was discussed earlier.

Potential Fe(II) binding sites (labile cation binding sites, in contrast to the integral copper binding sites) have been identified near the T1 copper atoms in domains 4 and 6 of human Cp as have the residues that likely coordinate the cationic species [100]. These Fe(II) ligands consist of a histidyl residue and three acidic residues. However, in domain 2 of human Cp, the complement of residues that should coordinate the labile cation differs and is composed of a tyrosyl residue, two glutamyl residues, and an asparagyl residue. Thus, it is thought that there is no Fe(II) binding site in domain 2 of human Cp, again providing evidence for the conclusion that the mononuclear copper in domain 2 may not function in the ferroxidase activity of human Cp. Human Hp also possesses similar amino acid residues in domains 4 and 6 that may function to coordinate the Fe(II) prior to oxidation. However, unlike human Cp, the residues in domain 2 of human Hp are comprised of a histidyl residue,

a seryl residue, and two glutamyl residues. These may facilitate binding of Fe(II) to the putative labile cation binding site. Mutants have been designed to perturb the predicted Fe(II) binding sites in domains 2, 4, and 6 of recombinant human Hp. Ferroxidase and amine oxidase activities of the recombinant mutant Hp proteins could be assessed as described previously.

Very recently, it has been shown that CueO, Fet3, and Cp have cuprous oxidase activity (enzymatic conversion of Cu(I) to Cu(II)) in addition to ferroxidase activity [41, 101]. Based on the sequential and proposed structural similarities of Hp and Cp, recombinant human Hp will likely possesses cuprous oxidase activity. It will be of interest to determine if the mutations described in Table 4.2 will also affect the putative cuprous oxidase activity. As a crystal structure of Hp is not yet available and the coordinates for the model of the ectodomain of Hp [58] were not made publicly available, it is hoped that the aforementioned mutants will elucidate some of the details of the electron transfer pathways, the importance of the methionyl residue as a ligand for the T1 copper atom in domain 2, and the Fe(II) binding sites. We are currently attempting crystallization screens for subsequent structure determination of Hp in collaboration with Dr. Natalie Strynadka's laboratory (University of British Columbia, Canada). We realize that the carbohydrate moieties present on Hp may make obtaining crystals difficult and, if necessary, we are prepared to treat Hp with glycosidases. However, the blue colour of Hp should facilitate crystal identification during the screens. A structural model of Hp will complement the existing structures for human Cp [36] and *S. cerevisiae* Fet3p [96].

Table 4.2 Amino acid residues of human Hp that may contribute to integral copper coordination, electron transfer, and labile cation binding. These are based on Appendix A and the crystal structure of human Cp [100]. Mutants have been generated as shown but the constructs have not yet been transfected into BHK cells for expression.

Human Hp Residues*	Location of Residues in Human Hp	Proposed Function in Human Hp	Mutation(s) in Recombinant Human Hp
M357	domain 2	ligand for mononuclear T1 copper	M357L
E264/H269	domain 2	coordinate Fe(II) prior to oxidation	E264A/H269A
D616/H621	domain 4	coordinate Fe(II) prior to oxidation	D616A/H621A
E960/H965	domain 6	coordinate Fe(II) prior to oxidation	E960A/H965A
E652	electron transfer pathway between domains 2 and 4	electron transfer from T1 copper in domain 2 to T1 copper in domain 4	E652A
D996	electron transfer pathway between domains 4 and 6	electron transfer from T1 copper in domain 4 to T1 copper in domain 6	D996A

*amino acid numbering is according to Appendix A

4.8 Significance of the Work

As demonstrated by disorders resulting from both iron overload and iron deficiency (some of which include Alzheimer's, Parkinson's, age-related macular degeneration, and anemias), iron homeostasis is essential for the well-being of humans. It is now becoming increasingly clear that copper and iron metabolism are intimately linked as individuals with

aceruloplasminemia have an anemia [102], as does the *sla* mouse [53, 57], and absence of both Hp and Cp in mouse leads to severe iron overloading in the retinal pigment epithelium [62].

Prior to the present work, the human Hp protein had not been isolated and characterized and the role of this protein in human iron homeostasis was unclear. By characterizing the recombinant protein and assessing its enzymatic activity, a clearer understanding of its potential role in iron homeostasis has been gained. These studies should open the way for further functional studies that can define the interaction of human Hp with other proteins involved in iron homeostasis (Fpn1 and Tf).

4.9 Conclusions

Although the *sla* disorder has been recognized since the 1960s [53], the discovery of Hp by Christopher Vulpe and his colleagues did not occur until nearly forty years later [57]. When this dissertation project was started in the middle of 2002, a PubMed search for "hephaestin" generated only 21 hits; it was exciting to start work on the expression and characterization of such a novel protein. To date, a modest 69 hits are returned from the aforementioned "hephaestin" search with the work from this dissertation offering the first insight into the metal binding and enzymatic properties of purified Hp, from a recombinant source or otherwise. The present work establishes that Hp, like Cp (from blood plasma) and Fet3p (from yeast), is a multicopper oxidase with ferroxidase activity. Moreover, this ferroxidase activity has now been shown to promote efficient loading of apo Tf with iron to form diferric Tf.

Bibliography

1. Harris, W. R. (2002). Iron chemistry *in* "Molecular and cellular iron transport" (D. M. Templeton, Ed.) pp. 1-40. Marcel Dekker Inc., New York.

2. Linder, M. C., Zerounian, N. R., Moriya, M., and Malpe, R. (2003). Iron and copper homeostasis and intestinal absorption using the Caco2 cell model. *Biometals.* 16, 145-60.

3. Aisen, P., Enns, C., and Wessling-Resnick, M. (2001). Chemistry and biology of eukaryotic iron metabolism. *Int J Biochem Cell Biol.* 33, 940-59.

4. Conrad, M. E., and Umbreit, J. N. (2000). Iron absorption and transport-an update. *Am J Hematol.* 64, 287-98.

5. Liochev, S. I., and Fridovich, I. (1994). The role of $O_2^{\cdot-}$ in the production of $HO^{\cdot}$: in vitro and in vivo. *Free Radic Biol Med.* 16, 29-33.

6. Bergamini, C. M., Gambetti, S., Dondi, A., and Cervellati, C. (2004). Oxygen, reactive oxygen species and tissue damage. *Curr Pharm Des.* 10, 1611-26.

7. Weinberg, E. D. (1997). The Lactobacillus anomaly: total iron abstinence. *Perspect Biol Med.* 40, 578-83.

8. Wandersman, C., and Delepelaire, P. (2004). Bacterial iron sources: from siderophores to hemophores. *Annu Rev Microbiol.* 58, 611-47.

9. Andrews, S. C., Robinson, A. K., and Rodriguez-Quinones, F. (2003). Bacterial iron homeostasis. *FEMS Microbiol Rev.* 27, 215-37.

10. Kosman, D. J. (2003). Molecular mechanisms of iron uptake in fungi. *Mol Microbiol.* 47, 1185-97.

11. Bonaccorsi di Patti, M. C., Miele, R., Eugenia Schinina, M., and Barra, D. (2005). The yeast multicopper oxidase Fet3p and the iron permease Ftr1p physically interact. *Biochem Biophys Res Commun.* 333, 432-7.

12. De Freitas, J., Wintz, H., Kim, J. H., Poynton, H., Fox, T., and Vulpe, C. (2003). Yeast, a model organism for iron and copper metabolism studies. *Biometals.* 16, 185-97.

13. Pufahl, R. A., Singer, C. P., Peariso, K. L., Lin, S. J., Schmidt, P. J., Fahrni, C. J., Culotta, V. C., Penner-Hahn, J. E., and O'Halloran, T. V. (1997). Metal ion chaperone function of the soluble Cu(I) receptor Atx1. *Science.* 278, 853-6.

14. Umbreit, J. (2005). Iron deficiency: a concise review. *Am J Hematol.* 78, 225-31.

15. McKie, A. T., Barrow, D., Latunde-Dada, G. O., Rolfs, A., Sager, G., Mudaly, E., Mudaly, M., Richardson, C., Barlow, D., Bomford, A., Peters, T. J., Raja, K. B., Shirali, S., Hediger, M. A., Farzaneh, F., and Simpson, R. J. (2001). An iron-regulated ferric reductase associated with the absorption of dietary iron. *Science.* 291, 1755-9.

16. Fleming, M. D., Trenor, C. C., 3rd, Su, M. A., Foernzler, D., Beier, D. R., Dietrich, W. F., and Andrews, N. C. (1997). Microcytic anaemia mice have a mutation in Nramp2, a candidate iron transporter gene. *Nat Genet.* 16, 383-6.

17. Gruenheid, S., Cellier, M., Vidal, S., and Gros, P. (1995). Identification and characterization of a second mouse Nramp gene. *Genomics.* 25, 514-25.

18. Gunshin, H., Mackenzie, B., Berger, U. V., Gunshin, Y., Romero, M. F., Boron, W. F., Nussberger, S., Gollan, J. L., and Hediger, M. A. (1997). Cloning and characterization of a mammalian proton-coupled metal-ion transporter. *Nature.* 388, 482-8.

19. Shayeghi, M., Latunde-Dada, G. O., Oakhill, J. S., Laftah, A. H., Takeuchi, K., Halliday, N., Khan, Y., Warley, A., McCann, F. E., Hider, R. C., Frazer, D. M., Anderson, G. J., Vulpe, C. D., Simpson, R. J., and McKie, A. T. (2005). Identification of an intestinal heme transporter. *Cell.* 122, 789-801.

20. McKie, A. T., and Barlow, D. J. (2004). The SLC40 basolateral iron transporter family (IREG1/ferroportin/MTP1). *Pflugers Arch.* 447, 801-6.

21. Fleming, R. E. (2005). Advances in understanding the molecular basis for the regulation of dietary iron absorption. *Curr Opin Gastroenterol.* 21, 201-6.

22. MacGillivray, R. T. A., and Mason, A. B. (2002). Transferrins *in* "Molecular and cellular iron transport" (D. M. Templeton, Ed.) pp. 41-69. Marcel Dekker Inc., New York.

23. Enns, C. A. (2002). The transferrin receptor *in* "Molecular and cellular iron transport" (D. M. Templeton, Ed.) pp. 71-94. Marcel Dekker, Inc, New York.

24. Ohgami, R. S., Campagna, D. R., Greer, E. L., Antiochos, B., McDonald, A., Chen, J., Sharp, J. J., Fujiwara, Y., Barker, J. E., and Fleming, M. D. (2005). Identification of a ferrireductase required for efficient transferrin-dependent iron uptake in erythroid cells. *Nat Genet.* 37, 1264-9.

25. Aisen, P. (1998). Transferrin, the transferrin receptor, and the uptake of iron by cells. *Met Ions Biol Syst.* 35, 585-631.

26. Ganz, T. (2003). Hepcidin, a key regulator of iron metabolism and mediator of anemia of inflammation. *Blood.* 102, 783-8.

27. Pigeon, C., Ilyin, G., Courselaud, B., Leroyer, P., Turlin, B., Brissot, P., and Loreal, O. (2001). A new mouse liver-specific gene, encoding a protein homologous to human antimicrobial peptide hepcidin, is overexpressed during iron overload. *J Biol Chem.* 276, 7811-9.

28. Frazer, D. M., and Anderson, G. J. (2003). The orchestration of body iron intake: how and where do enterocytes receive their cues? *Blood Cells Mol Dis.* 30, 288-97.

29. Nemeth, E., Tuttle, M. S., Powelson, J., Vaughn, M. B., Donovan, A., Ward, D. M., Ganz, T., and Kaplan, J. (2004). Hepcidin regulates cellular iron efflux by binding to ferroportin and inducing its internalization. *Science.* 306, 2090-3.

30. Yamaji, S., Sharp, P., Ramesh, B., and Srai, S. K. (2004). Inhibition of iron transport across human intestinal epithelial cells by hepcidin. *Blood.* 104, 2178-80.

31. Bratosin, D., Mazurier, J., Tissier, J. P., Estaquier, J., Huart, J. J., Ameisen, J. C., Aminoff, D., and Montreuil, J. (1998). Cellular and molecular mechanisms of senescent erythrocyte phagocytosis by macrophages. A review. *Biochimie.* 80, 173-95.

32. Zecca, L., Youdim, M. B., Riederer, P., Connor, J. R., and Crichton, R. R. (2004). Iron, brain ageing and neurodegenerative disorders. *Nat Rev Neurosci.* 5, 863-73.

33. Solomon, E. I., and Lowery, M. D. (1993). Electronic structure contributions to function in bioinorganic chemistry. *Science.* 259, 1575-81.

34. Sundaram, U. M., Zhang, H. H., Hedman, B., Hodgson, K. O., and Solomon, E. I. (1997). Spectroscopic investigation of peroxide binding to the trinuclear copper cluster site in laccase: correlation with the peroxy-level intermediate and relevance to catalysis. *J Am Chem Soc.* 119, 12525-40.

35. Solomon, E. I., Chen, P., Metz, M., Lee, S. K., and Palmer, A. E. (2001). Oxygen binding, activation, and reduction to water by copper proteins. *Angew Chem Int Ed Engl.* 40, 4570-90.

36. Zaitseva, I., Zaitsev, V. N., Card, G., Moshkov, K., Bax, B., Ralph, A., and Lindley, P. F. (1996). The X-ray structure of human serum ceruloplasmin at 3.1 Å: nature of the copper centres. *J Biol Inorg Chem.* 1, 15-23.

37. Grass, G., and Rensing, C. (2001). CueO is a multi-copper oxidase that confers copper tolerance in Escherichia coli. *Biochem Biophys Res Commun.* 286, 902-8.

38. de Silva, D. M., Askwith, C. C., Eide, D., and Kaplan, J. (1995). The FET3 gene product required for high affinity iron transport in yeast is a cell surface ferroxidase. *J Biol Chem.* 270, 1098-101.

39. Osaki, S., Johnson, D. A., and Frieden, E. (1966). The possible significance of the ferrous oxidase activity of ceruloplasmin in normal human serum. *J Biol Chem.* 241, 2746-51.

40. Roberts, S. A., Weichsel, A., Grass, G., Thakali, K., Hazzard, J. T., Tollin, G., Rensing, C., and Montfort, W. R. (2002). Crystal structure and electron transfer kinetics of CueO, a multicopper oxidase required for copper homeostasis in *Escherichia coli. Proc Natl Acad Sci U S A.* 99, 2766-71.

41. Singh, S. K., Grass, G., Rensing, C., and Montfort, W. R. (2004). Cuprous oxidase activity of CueO from *Escherichia coli. J Bacteriol.* 186, 7815-7.

42. de Silva, D., Davis-Kaplan, S., Fergestad, J., and Kaplan, J. (1997). Purification and characterization of Fet3 protein, a yeast homologue of ceruloplasmin. *J Biol Chem.* 272, 14208-13.

43. Machonkin, T. E., and Solomon, E. I. (2000). The thermodynamics, kinetics, and molecular mechanism of intramolecular electron transfer in human ceruloplasmin. *J Am Chem Soc.* 122, 12547-60.

44. Rulisek, L., Solomon, E. I., and Ryde, U. (2005). A combined quantum and molecular mechanical study of the O2 reductive cleavage in the catalytic cycle of multicopper oxidases. *Inorg Chem.* 44, 5612-28.

45. Kroneck, P. M. H. (1997). Redox properties of blue multi-copper oxidases *in* "Multi-copper oxidases" (A. Messerschmidt, Ed.) pp. 391-407. World Scientific Publishing Co. Pte. Ltd., River Edge.

46. Machonkin, T. E., Zhang, H. H., Hedman, B., Hodgson, K. O., and Solomon, E. I. (1998). Spectroscopic and magnetic studies of human ceruloplasmin: identification of a redox-inactive reduced Type 1 copper site. *Biochemistry.* 37, 9570-8.

47. Gray, H. B., Malmstrom, B. G., and Williams, R. J. (2000). Copper coordination in blue proteins. *J Biol Inorg Chem.* 5, 551-9.

48. Stephens, P. J., Jollie, D. R., and Warshel, A. (1996). Protein control of redox potentials of iron-sulfur proteins. *Chem Rev.* 96, 2491-514.

49. Machonkin, T. E., Quintanar, L., Palmer, A. E., Hassett, R., Severance, S., Kosman, D. J., and Solomon, E. I. (2001). Spectroscopy and reactivity of the type 1 copper site in Fet3p from *Saccharomyces cerevisiae*: correlation of structure with reactivity in the multicopper oxidases. *J Am Chem Soc.* 123, 5507-17.

50. Bonomi, F., Kurtz, J., D.M., and Cui, X. (1996). Ferroxidase activity of recombinant *Desulfovibrio vulgaris* rubrerythrin. *J Biol Inorg Chem.* 1, 67-72.

51. Brown, M. A., Stenberg, L. M., and Mauk, A. G. (2002). Identification of catalytically important amino acids in human ceruloplasmin by site-directed mutagenesis. *FEBS Lett.* 520, 8-12.

52. Hellman, N. E., and Gitlin, J. D. (2002). Ceruloplasmin metabolism and function. *Annu Rev Nutr.* 22, 439-58.

53. Falconer, D. S., and Isaacson, J. H. (1962). The genetics of sex-linked anemia in the mouse. *Genet. Res., Camb.* 3, 248-50.

54. Bannerman, R. M., and Cooper, R. G. (1966). Sex-linked anemia: a hypochromic anemia of mice. *Science.* 151, 581-2.

55. Edwards, J. A., and Bannerman, R. M. (1970). Hereditary defect of intestinal iron transport in mice with sex-linked anemia. *J Clin Invest.* 49, 1869-71.

56. Manis, J. (1971). Intestinal iron-transport defect in the mouse with sex-linked anemia. *Am J Physiol.* 220, 135-9.

57. Vulpe, C. D., Kuo, Y. M., Murphy, T. L., Cowley, L., Askwith, C., Libina, N., Gitschier, J., and Anderson, G. J. (1999). Hephaestin, a ceruloplasmin homologue implicated in intestinal iron transport, is defective in the *sla* mouse. *Nat Genet.* 21, 195-9.

58. Syed, B. A., Beaumont, N. J., Patel, A., Naylor, C. E., Bayele, H. K., Joannou, C. L., Rowe, P. S., Evans, R. W., and Srai, S. K. (2002). Analysis of the human hephaestin gene and protein: comparative modelling of the N-terminus ecto-domain based upon ceruloplasmin. *Protein Eng.* 15, 205-14.

59. Frazer, D. M., Vulpe, C. D., McKie, A. T., Wilkins, S. J., Trinder, D., Cleghorn, G. J., and Anderson, G. J. (2001). Cloning and gastrointestinal expression of rat hephaestin: relationship to other iron transport proteins. *Am J Physiol Gastrointest Liver Physiol.* 281, G931-9.

60. Chen, H., Attieh, Z. K., Su, T., Syed, B. A., Gao, H., Alaeddine, R. M., Fox, T. C., Usta, J., Naylor, C. E., Evans, R. W., McKie, A. T., Anderson, G. J., and Vulpe, C. D. (2004). Hephaestin is a ferroxidase that maintains partial activity in sex-linked anemia mice. *Blood.* 103, 3933-9.

61. Kuo, Y. M., Su, T., Chen, H., Attieh, Z., Syed, B. A., McKie, A. T., Anderson, G. J., Gitschier, J., and Vulpe, C. D. (2004). Mislocalisation of hephaestin, a multicopper ferroxidase involved in basolateral intestinal iron transport, in the sex linked anaemia mouse. *Gut.* 53, 201-6.

62. Hahn, P., Qian, Y., Dentchev, T., Chen, L., Beard, J., Harris, Z. L., and Dunaief, J. L. (2004). Disruption of ceruloplasmin and hephaestin in mice causes retinal iron overload and retinal degeneration with features of age-related macular degeneration. *Proc Natl Acad Sci U S A.* 101, 13850-5.

63. Li, L., Vulpe, C. D., and Kaplan, J. (2003). Functional studies of hephaestin in yeast: evidence for multicopper oxidase activity in the endocytic pathway. *Biochem J.* 375, 793-8.

64. Bielli, P., Bellenchi, G. C., and Calabrese, L. (2001). Site-directed mutagenesis of human ceruloplasmin: production of a proteolytically stable protein and structure-activity relationships of type 1 sites. *J Biol Chem.* 276, 2678-85.

65. Bonaccorsi di Patti, M. C., Bellenchi, G. C., Bielli, P., and Calabrese, L. (1999). Release of highly active Fet3 from membranes of the yeast *Pichia pastoris* by limited proteolysis. *Arch Biochem Biophys.* 372, 295-9.

66. Hassett, R. F., Yuan, D. S., and Kosman, D. J. (1998). Spectral and kinetic properties of the Fet3 protein from *Saccharomyces cerevisiae*, a multinuclear copper ferroxidase enzyme. *J Biol Chem.* 273, 23274-82.

67. Galli, I., Musci, G., and Bonaccorsi di Patti, M. C. (2004). Sequential reconstitution of copper sites in the multicopper oxidase CueO. *J Biol Inorg Chem.* 9, 90-5.

68. Sambrook, J., and Russell, D. W. (2001) *Molecular cloning : a laboratory manual*, 3rd ed., Cold Spring Harbor Laboratory Press, Cold Spring Harbor, N.Y.

69. Evan, G. I., Lewis, G. K., Ramsay, G., and Bishop, J. M. (1985). Isolation of monoclonal antibodies specific for human c-myc proto-oncogene product. *Mol Cell Biol.* 5, 3610-6.

70. Chen, C., and Okayama, H. (1987). High-efficiency transformation of mammalian cells by plasmid DNA. *Mol Cell Biol.* 7, 2745-52.

71. Molday, R. S., and MacKenzie, D. (1983). Monoclonal antibodies to rhodopsin: characterization, cross-reactivity, and application as structural probes. *Biochemistry.* 22, 653-60.

72. Hodges, R. S., Heaton, R. J., Parker, J. M., Molday, L., and Molday, R. S. (1988). Antigen-antibody interaction. Synthetic peptides define linear antigenic determinants recognized by monoclonal antibodies directed to the cytoplasmic carboxyl terminus of rhodopsin. *J Biol Chem.* 263, 11768-75.

73. Palmiter, R. D., Behringer, R. R., Quaife, C. J., Maxwell, F., Maxwell, I. H., and Brinster, R. L. (1987). Cell lineage ablation in transgenic mice by cell-specific expression of a toxin gene. *Cell.* 50, 435-43.

74. Garratt, R. C., Evans, R. W., Hasnain, S. S., Lindley, P. F., and Sarra, R. (1991). X.a.f.s. studies of chicken dicupric ovotransferrin. *Biochem J.* 280 (Pt 1), 151-5.

75. Li, H., Sadler, P. J., and Sun, H. (1996). Unexpectedly strong binding of a large metal ion (Bi^{3+}) to human serum transferrin. *J Biol Chem.* 271, 9483-9.

76. Mason, A. B., Miller, M. K., Funk, W. D., Banfield, D. K., Savage, K. J., Oliver, R. W., Green, B. N., MacGillivray, R. T., and Woodworth, R. C. (1993). Expression of glycosylated and nonglycosylated human transferrin in mammalian cells. Characterization of the recombinant proteins with comparison to three commercially available transferrins. *Biochemistry.* 32, 5472-9.

77. Griffiths, T. A., Mauk, A. G., and MacGillivray, R. T. (2005). Recombinant expression and functional characterization of human hephaestin: a multicopper oxidase with ferroxidase activity. *Biochemistry.* 44, 14725-31.

78. Solomon, E. I., Sundaram, U. M., and Machonkin, T. E. (1996). Multicopper oxidases and oxygenases. *Chem Rev.* 96, 2563-606.

79. Smith, C. A., Anderson, B. F., Baker, H. M., and Baker, E. N. (1992). Metal substitution in transferrins: the crystal structure of human copper-lactoferrin at 2.1- Å resolution. *Biochemistry.* 31, 4527-33.

80. Musci, G., Di Marco, S., Bellenchi, G. C., and Calabrese, L. (1996). Reconstitution of ceruloplasmin by the Cu(I)-glutathione complex. Evidence for a role of Mg^{2+} and ATP. *J Biol Chem.* 271, 1972-8.

81. Roy, C. N., and Enns, C. A. (2000). Iron homeostasis: new tales from the crypt. *Blood.* 96, 4020-7.

82. Patel, B. N., and David, S. (1997). A novel glycosylphosphatidylinositol-anchored form of ceruloplasmin is expressed by mammalian astrocytes. *J Biol Chem.* 272, 20185-90.

83. Funk, W. D., MacGillivray, R. T., Mason, A. B., Brown, S. A., and Woodworth, R. C. (1990). Expression of the amino-terminal half-molecule of human serum transferrin in cultured cells and characterization of the recombinant protein. *Biochemistry.* 29, 1654-60.

84. Guarna, M. M., Cote, H. C., Kwan, E. M., Rintoul, G. L., Meyhack, B., Heim, J., MacGillivray, R. T., Warren, R. A., and Kilburn, D. G. (2000). Factor X fusion proteins: improved production and use in the release in vitro of biologically active hirudin from an inactive alpha-factor-hirudin fusion protein. *Protein Expr Purif.* 20, 133-41.

85. Kingston, I. B., Kingston, B. L., and Putnam, F. W. (1977). Chemical evidence that proteolytic cleavage causes the heterogeneity present in human ceruloplasmin preparations. *Proc Natl Acad Sci U S A.* 74, 5377-81.

86. Dwulet, F. E., and Putnam, F. W. (1981). Complete amino acid sequence of a 50,000-dalton fragment of human ceruloplasmin. *Proc Natl Acad Sci U S A.* 78, 790-4.

87. Ryden, L. (1971). Evidence for proteolytic fragments in commercial samples of human ceruloplasmin. *FEBS Lett.* 18, 321-5.

88. Pace, C. N., Vajdos, F., Fee, L., Grimsley, G., and Gray, T. (1995). How to measure and predict the molar absorption coefficient of a protein. *Protein Sci.* 4, 2411-23.

89. Ryden, L., and Bjork, I. (1976). Reinvestigation of some physicochemical and chemical properties of human ceruloplasmin (ferroxidase). *Biochemistry.* 15, 3411-7.

90. Boivin, S., Aouffen, M., Fournier, A., and Mateescu, M. A. (2001). Molecular characterization of human and bovine ceruloplasmin using MALDI-TOF mass spectrometry. *Biochem Biophys Res Commun.* 288, 1006-10.

91. Nittis, T., and Gitlin, J. D. (2004). Role of copper in the proteosome-mediated degradation of the multicopper oxidase hephaestin. *J Biol Chem.* 279, 25696-702.

92. Julenius, K., Molgaard, A., Gupta, R., and Brunak, S. (2005). Prediction, conservation analysis, and structural characterization of mammalian mucin-type O-glycosylation sites. *Glycobiology.* 15, 153-64.

93. Machonkin, T. E., Musci, G., Zhang, H. H., Bonaccorsi di Patti, M. C., Calabrese, L., Hedman, B., Hodgson, K. O., and Solomon, E. I. (1999). Investigation of the anomalous spectroscopic features of the copper sites in chicken ceruloplasmin: comparison to human ceruloplasmin. *Biochemistry.* 38, 11093-102.

94. Guzzi, R., Milardi, D., La Rosa, C., Grasso, D., Verbeet, M. P., Canters, G. W., and Sportelli, L. (2003). The effect of copper/zinc replacement on the folding free energy of wild type and Cys3Ala/Cys26Ala azurin. *Int J Biol Macromol.* 31, 163-70.

95. Klemens, F. K., Severns, J. C., Tamilarasan, R., and McMillin, D. R. (1996). Aspects of the demetalation and remetalation of ceruloplasmin. *Inorganica Chimica Acta.* 250, 75-9.

96. Taylor, A. B., Stoj, C. S., Ziegler, L., Kosman, D. J., and Hart, P. J. (2005). The copper-iron connection in biology: structure of the metallo-oxidase Fet3p. *Proc Natl Acad Sci U S A.* 102, 15459-64.

97. Osaki, S. (1966). Kinetic studies of ferrous ion oxidation with crystalline human ferroxidase (ceruloplasmin). *J Biol Chem.* 241, 5053-9.

98. Askwith, C. C., and Kaplan, J. (1998). Site-directed mutagenesis of the yeast multicopper oxidase Fet3p. *J Biol Chem.* 273, 22415-9.

99. Rae, T. D., Schmidt, P. J., Pufahl, R. A., Culotta, V. C., and O'Halloran, T. V. (1999). Undetectable intracellular free copper: the requirement of a copper chaperone for superoxide dismutase. *Science.* 284, 805-8.

100. Lindley, P. F., Card, G., Zaitseva, I., Zaitsev, V. N., Reinhammar, B., Selin-Lindgren, E., and Yoshida, K. (1997). An X-ray structural study of human ceruloplasmin in relation to ferroxidase activity. *J Biol Inorg Chem.* 2, 454-63.

101. Stoj, C., and Kosman, D. J. (2003). Cuprous oxidase activity of yeast Fet3p and human ceruloplasmin: implication for function. *FEBS Lett.* 554, 422-6.

102. Harris, Z. L., Takahashi, Y., Miyajima, H., Serizawa, M., MacGillivray, R. T., and Gitlin, J. D. (1995). Aceruloplasminemia: molecular characterization of this disorder of iron metabolism. *Proc Natl Acad Sci U S A.* 92, 2539-43.

Appendix A: Sequence Alignment of the Multicopper Oxidases Hephaestin and Ceruloplasmin

Sequences of human Hp (hHp) and human Cp (hCp) were aligned using the ClustalW multiple sequence alignment tool from the European Bioinformatics Institute available online at http://www.ebi.ac.uk/clustalw/. Conserved residues are denoted with *. Residues acting as ligands for integral Type 1, 2, or 3 copper atoms are denoted with a 1, 2, or 3. Cysteinyl residues participating in disulfide bond formation are denoted with DS. Residues that render Cp susceptible to proteolytic degradation are underlined.

```
                ------signal peptide-----
                |                    |
hHp             MESGHLLWALLFMQSLWPQLTDGATRVYYLGIRDVQWNYAPKGRNVITNQPLDSDIVAS- 59
hCp             --MKILILGIFLFLCSTPAWAK--EKHYYIGIIETTWDYASDHG---EKKLISVDTEHSN 53
                     *           *         ** **    * **               *   *


hHp             SFLKSDKNRIGGTYKKTIYKEYKDDSYTDEVAQPAWLGFLGPVLQAEVGDVILIHLKNFA 119
hCp             IYLQNGPDRIGRLYKKALYLQYTDETFRTTIEKPVWLGFLGPIIKAETGDKVYVHLKNLA 113
                  *    ***  ***  *  * *          * *******   ** **    **** *

                     2 3
hHp             TRPYTIHPHGVFYEKDSEGSLYPDGSSGPLKADDSVPPGGSHIYNWTIPEGHAPTDADPA 179
hCp             SRPYTFHSHGITYYKEHEGAIYPDNTTDFQRADDKVYPGEQYTYMLLATEEQSPGEGDGN 173
                 **** * **  * *  **  ***       *** * **    *     *   *   *

                DS    3 3                  DS
hHp             CLTWIYHSHVDAPRDIATGLIGPLITCKRGALDGNSPPQRQDVDHDFFLLFSVVDENLSW 239
hCp             CVTRIYHSHIDAPKDIASGLIGPLIICKKDSLDKE---KEKHIDREFVVMFSVVDENFSW 230
                * * ***** *** *** ******* **   **          *  *   ******* **

                                                          DS
hHp             HLNENIATYCSDPASVDKEDETFQESNRMHAINGFVFGNLPELNMCAQKRVAWHLFGMGN 299
hCp             YLEDNIKTYCSEPEKVDKDNEDFQESNRMYSVNGYTFGSLPGLSMCAEDRVKWYLFGMGN 290
                 *  ** **** *  ***  * *******   **  ** ** * ***  ** * ******

                   1                                          1    1    1
hHp             EIDVHTAFFHGQMLTTRGHHTDVANIFPATFVTAEMVPWEPGTWLISCQVNSHFRDGMQA 359
hCp             EVDVHAAFFHGQALTNKNYRIDTINLFPATLFDAYMVAQNPGEWMLSCQNLNHLKAGLQA 350
                * *** ****** **       *  * ****   * **   ** *  ***   *   * **

                     DS
hHp             LYKVKSCSMAPPVDLLTGK-VRQYFIEAHEIQWDYGPMGHDGSTGKNLREPGSISDKFFQ 418
hCp             FFQVQECNKSSSKDNIRGKHVRHYYIAAEEIIWNYAPSGIDIFTKENLTAPGSDSAVFFE 410
                   *  *       *   ** ** * * * ** * * * * *  *  **  *** *  **


hHp             KSSSRIGGTYWKVRYEAFQDETFQEKMHLE-EDRHLGILGPVIRAEVGDTIQVVFYNRAS 477
hCp             QGTTRIGGSYKKLVYREYTDASFTNRKERGPEEEHLGILGPVIWAEVGDTIRVTFHNKGA 470
                    **** * *  *    *  *         *  ********* ******* * * *


hHp             QPFSMQPHGVFYEKDYEGTVYN-----DGSSYP--GLVAKPFEKVTYRWTVPPHAGPTAQ 530
hCp             YPLSIEPIGVRFNKNNEGTYYSPNYNPQSRSVPPSASHVAPTETFTYEWTVPKEVGPTNA 530
                 * *  * **   *  *** *         * *       * *  ** **** *** 

                  DS                         DS
hHp             DPACLTWMYFSAADPIRDTNSGLVGPLLVCRAGALGADGKQKGVDKEFFLLFTVLDENKS 590
hCp             DPVCLAKMYYSAVDPTKDIFTGLIGPMKICKKGSLHANGRQKDVDKEFYLFPTVFDENES 590
                ** **  ** ** **  *   ** **   *  * * * * ** ***** *  ** *** *
```

```
                                                                DS
hHp             WYSNANQAAAMLDFRLLSEDIEGFQDSNRMHAINGFLFSNLPRLDMCKGDTVAWHLLGLG 650
hCp             LLLEDNIRMFTTAPDQVDKEDEDFQESNKMHSMNGFMYGNQPGLTMCKGDSVVWYLFSAG 650
                     *                * ** ** **  ***   * * * ***** * * *   *


                    1                                                1    1    1
hHp             TETDVHGVMFQGNTVQLQGMRKGAAMLFPHTFVMAIMQPDNLGTFEIYCQAGSHREAGMR 710
hCp             NEADVHGIYFSGNTYLWRGERRDTANLFPQTSLTLHMWPDTEGTFNVECLTTDHYTGGMK 710
                 * **** * ***    * *   * *** *     * **  ***   *    *   **

                      DS
hHp             AIYNVSQCPGHQATPRQRYQAARIYYIMAEEVEWDYCPDRSWEREWHNQSEKDSYGYIFL 770
hCp             QKYTVNQCR-RQSEDSTFYLGERTYYIAAVEVEWDYSPQREWEKELHHLQEQN-VSNAFL 768
                  * * **   *       *   * *** * ****** * * ** * *   *       **


hHp             SNKDGLLGSRYKKAVFREYTDGTFRIPRPRTGPEEHLGILGPLIKGEVGDILTVVFKNNA 830
hCp             DKGEFYIGSKYKKVVYRQYTDSTFRVPVERKAEEEHLGILGPQLHADVGDKVKIIFKNMA 828
                       ** *** * * *** *** *  *   *********      ***     *** *


                                                            DS
hHp             SRPYSVHAHGVL-ESTTVWPLAAEPGEVVTYQWNIPERSGPGPNDSACVSWIYYSAVDPI 889
hCp             TRPYSIHAHGVQTESSTVTP--TLPGETLTYVWKIPERSGAGTEDSACIPWAYYSTVDQV 886
                 **** *****  ** ** *    ***  ** * ****** *  ****  * *** **

                    DS
hHp             KDMYSGLVGPLAICQKGILEPHGGRSDMDREFALLFLIFDENKSWYLEENVATHGSQDPG 949
hCp             KDLYSGLIGPLIVCRRPYLKVFNPRR--KLEFALLFLVFDENESWYLDDNIKTY-SDHPE 943
                ** **** ***  *    *     *     ******* **** ****  *  *  *  *


                                                                1  2 3
hHp             SINLQDETFLESNKMHAINGKLYANLRGLTMYQGERVAWYMLAMGQDVDLHTIHFHAESF 1009
hCp             KVNKDDEEFIESNKMHAINGRMFGNLQGLTMHVGDEVNWYLMGMGNEIDLHTVHFHGHSF 1003
                  *  ** * **********    ** ****  *  * **   **   **** ***  **


                                           313   1    1
hHp             LYRNGENYRADVVDLFPGTFEVVEMVASNPGTWLMHCHVTDHVHAGMETLFTVFSRTEHL 1069
hCp             QYKHRGVYSSDVFDIFPGTYQTLEMFPRTPGIWLLHCHVTDHIHAGMETTYTVLQNEDTK 1063
                 *     *  ** * ****    **    ** ** ******* ******  **


                                                -transmembrane region-
                                                |                    |
hHp             SPLTVITKETEKAVPPRDIEEGNVKMLGMQIPIKNVEMLASVLVAISVTLLLVVLALGGV 1129
hCp             SG------------------------------------------------------------ 1065
                *

hHp             VWYQHRQRKLRRNRRSILDDSFKLLSFKQ 1158
hCp             ------------------------------
```

The NCBI accession numbers for the preceding sequences are NP_620074 (for hHp) and AAA51976 (for hCp).